VOLUME I

FLOW LOSSES IN FLEXIBLE HOSE

FINAL REPORT

Contract NAS 9-4630

September, 1966

Approved by:

Charles A. Whitehurst
Principal Investigator

Bernard S. Pressburg
Co-Principal Investigator

Prepared by:

Kenneth L. Riley
Graduate Research Assistant

John R. Langley
Graduate Research Assistant

TABLE OF CONTENTS

VOLUME I

TABLE OF CONTENTS (CONTD.)

SUMMARY

A contract was awarded Louisiana State University on June 14, 1965, by the Manned Spacecraft Center, Houston, Texas for the purpose of investigating Flow Losses in Flexible Hose. The work was under the direction of Dr. Charles A. Whitehurst of the Department of Mechanical and Aerospace Engineering and Dr. Bernard S. Pressburg of the Chemical Engineering Department. Experimental work was carried out by graduate students from these departments. Other members of the engineering faculty and the Division of Engineering Research contributed knowledge and advice to the completion of the project.

Statement of work:

The primary objective of this investigation was to develop an empirical method for predicting flow losses in flexible hose. Specific objectives for the contractor were set forth in the contract as follows:

1. Determine an empirical method for predicting flow losses in flexible hose while using a gas and a liquid as the test mediums and considering:

    a. The effect of straight sections and bending

    b. Hose characteristics such as types of material and convolutions, convolutions/unit length, convolution height, diameter, bend angle, bend radius, bend radius to diameter ratio, effective roughness factor, effective roughness to diameter ratio, Reynolds number and friction factor.

2. Obtain an adequate quantity of data so correlation of results may be achieved in a reliable and comprehensive manner.

Further it was stated that all tests were to be performed under standard conditions utilizing air and water as the two (2) test mediums. The hose to be tested included:

1. Annular - both open and closed pitch convolutions were to be used.

2. Helical

Other criteria were:

1. Flexible hose diameters shall range from 1/2" to 3" inclusive.

2. Reynolds numbers shall range from 10^3 to maximum attainable.

3. Bend angles (Θ) shall vary from 0° to 180° inclusive with tests being performed at a sufficient number of standard intermediate angles so as to comply with Objective 2.

4. All test data used shall consist of the mean of at least three (3) runs per test set-up.

5. All other criteria shall be subject to Manned Spacecraft Center (MSC) approval.

Accomplishments:

The objectives of the research were accomplished in that: (1) the geometric parameters of the hose were investigated over the proposed flow rate ranges for the air and water systems, and (2) correlations relating friction factor and Reynolds number were derived which gave satisfactory agreement between the values predicted and those measured. For the water and air system the final equation is of the form:

$$f = \alpha Re^{\beta}$$

where α is a constant for any one hose. It can be calculated as a function of hose geometry. β is a second constant, the value of which also depends on the hose geometry. The correlations for α and β are:

1. Water system (annular hose)

$$\alpha = 0.01588\left(\frac{\lambda - \sigma}{\epsilon}\right) - 0.00215 \qquad (1)$$

2. Water system (helical hose)

$$\alpha = 0.02916\left(\frac{\lambda-\sigma}{\epsilon}\right) - 0.00886 \tag{1a}$$

3. Air system (annular hose)

$$\alpha = 0.02202\left(\frac{\lambda-\sigma}{\epsilon}\right) - 0.00287 \tag{1b}$$

4. Air system (helical hose)

$$\alpha = 0.04306\left(\frac{\lambda-\sigma}{\epsilon}\right) - 0.01318 \tag{1c}$$

5. Air and water systems (annular and helical)

$$\beta = 0.2987\left(\frac{\sigma\epsilon}{\lambda^2}\right) - 0.0313 \tag{2}$$

Figure 1 shows the various dimensions and nomenclature used in Equation (1) and (2). D is the minimum diameter (inside), λ is the pitch of the convolutions, and σ and ϵ are defined as shown. The bend angle correlation for the air and water systems was found to be:

$$\frac{f}{f_o} = 1.0 + 7.898\left(\frac{D}{R_B}\right)^{0.896} \tag{2a}$$

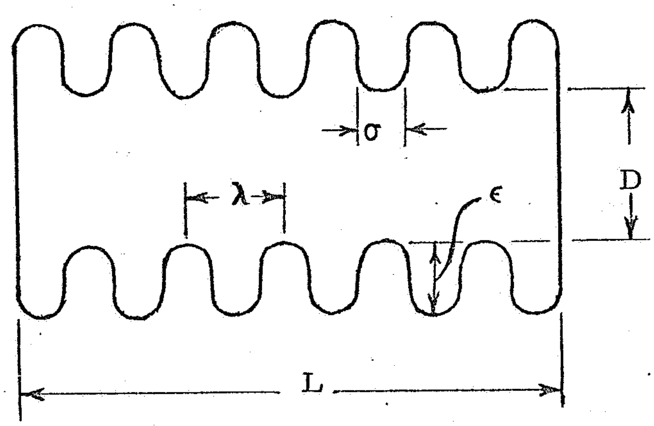

Figure 1. Hose Nomenclature

INTRODUCTION

Despite the widespread use of flexible hose - in space-oriented work and elsewhere - their selection and use is essentially an art. Information on the performance of one hose is of little or no value in predicting the performance of another hose of different size or of different geometric design. As can be seen in the literature survey below, existing data are fragmentary. They are not adequate for yielding a generalized correlation that could be used to predict with reasonable accuracy the performance of any type or size hose in a specific installation.

Literature survey:

This summary presents the pertinent results of a literature survey initiated in July 1965. A list of the papers and reports investigated is included as Appendix I of this report.

1. Smooth tubes

Correlations for the friction factor in smooth pipes are presented first in that they represent a limiting case of flexible pipe - i.e. zero corrugation height and pitch. Thus, their manner of behavior and the techniques used to handle them should provide guidance for the more complex case of corrugated pipe.

It will be noted that, unless specification is made to the contrary, the friction factors cited in this section are those of Blasius* defined:

$$f = \frac{\Delta P 2 g_c D}{L V^2 \rho} \tag{3}$$

Many empirical formulae have been proposed to represent the friction factor for smooth tubes over all or part of the range of Reynolds numbers up to as high as $R = 10^8$. Practically all have the form:

---

* As opposed to the Fanning friction factor which is one-fourth the Blasius value:

$$f_F = \frac{\Delta P 2 g_c D}{4 L V^2 \rho}$$

$$f = A + \frac{B}{R^n}, \tag{4}$$

the constants A, B, and n being adjusted to fit various sets of experimental results. Blasius published an equation to cover the Reynolds number range from 3000 to 100,000. It is:

$$f = \frac{0.3164}{R^{0.25}} \tag{5}$$

The equation

$$f = 0.0072 + \frac{0.6104}{R^{0.35}} \tag{6}$$

was proposed by Ch. H. Lees to represent the data of Stanton and Pannell which extended from R = 2500 to R = 430,000 approximately. M. Jakob and S. Erk published essentially the same formula in connection with their experiments which covered the range R = 85,000 to R = 470,000 approximately.

L. Schiller reported experiments made under his direction by R. Hermann at the Physikalischen Institut Leipsig. Here Schiller proposed the formula

$$f = 0.00540 + \frac{0.396}{R^{0.300}} \tag{7}$$

The range of measurement was from R = 20,000 to R = 1,900,000 and the formula was reported to fit the results within ±0.5 per cent.

Probably the most suitable single equation yet proposed is the one by E. C. Koo

$$f = 0.00560 + \frac{0.500}{R^{0.32}} \tag{8}$$

It represents the single friction factor for smooth tubes over the range of Reynolds numbers 3,000 to 3,000,000. A notable contribution to the knowledge of turbulent flow was made by Von Karman in an equation of the form

$$\frac{1}{\sqrt{f_{max}}} = A \log R_{max} \sqrt{f_{max}} + B \qquad (9)$$

wherein $R_{max} = \frac{\bar{v}_{max} \cdot d}{\upsilon}$, and $\bar{v}_{max}$ is the maximum velocity in the pipe. This equation represents the friction factors only when the effect of viscosity has become negligibly small.

Based on theory by Prandtl, Nikuradse showed that the equation of Von Karman could also be written

$$\frac{1}{\sqrt{f}} = A \log R \cdot \sqrt{f} + B, \qquad (10)$$

where $R = \frac{\bar{v}d}{\upsilon}$ and $\bar{v}$ is the average velocity instead of the less convenient maximum velocity.

Two sets of constants were proposed,

$$\frac{1}{\sqrt{f_F}} = 2.0 \log R\sqrt{f_F} - 0.8 \qquad (11)$$

which fit the plotted points over a very wide range of the variables and

$$\frac{1}{\sqrt{f}} = 1.95 \log R\sqrt{f} - 0.55 \qquad (12)$$

which seemed to be in better agreement with an analysis based on the maximum velocity.

Nikuradse concluded that the Blasius equation (5) represented the friction factors over the range of turbulent flow in which the effect of viscosity is important and placed the upper limit of this at about R = 100,000.

Above this value the viscosity seemed to have a negligible influence on the flow and Von Karman's equation using the constants (I) given previously would apply over a wide range, possibly up to $R = \infty$.

Since the Von Karman equation can be solved for f when R is known, only by successive approximations, Nikuradse proposed the empirical formula

$$f = 0.0032 + \frac{0.221}{R^{0.237}} \tag{13}$$

to represent the friction factors from $R = 10^5$ to $R = 10^8$.

2. Friction Factors in Corrugated Hose

Reliable published data on flow losses in flexible hose are limited in that the little data presented primarily deals with straight hose. Bend angle effects and other topological consideration have been neglected to a great extent. What data are available show wide variation in the correlations of the different investigations.

A. H. Gibson (1) gave the results of experiments on a pipe of 2.0 in. maximum bore, 1.8 in. minimum bore, and 0.4 in. pitch of corrugations. He observed that the loss of head was proportional to the mean velocity raised to an index greater than two. By dimensional analysis he then argued that this would lead to the apparently paradoxical result that an increase of viscosity would cause a decrease in the loss of head at a given rate of discharge. Further tests which he performed using water at two different temperatures in the corrugated pipe confirmed these deductions.

Webster and Metcalf (2) performed experiments on corrugated pipes having diameters 3, 5 and 7 feet. They found that a maximum value of f was reached, after which f decreased with increasing Reynolds number.

Neill (3) gives an analysis of previous results and after completing an experimental investigation into the losses in "standard" corrugated piping having a minimum diameter of 15 in. with corrugations 1/2 in. deep, and 2 2/3 in. pitch, suggests the formula

$$f = 0.16 (K_c/D)^{1/2} \tag{14}$$

where K_c is the depth of the corrugations, D is the minimum diameter of the pipe, and f is the friction factor in the expression for the loss of head.

$$h = \frac{flv^2}{2gD} \tag{15}$$

In taking pressure measurements, two of the tapping points for pressure measurement were situated at the crest of the corrugations and two at the trough, for each section where the pressure was recorded.

From figure 4 of Neill's work it is seen that the index of the mean velocity v in the equation

$$h = kv^n \tag{16}$$

is approximately 2.31 over the upper portion of the velocity range. Alternately, the value 2.423 was derived from a statistical analysis using the method of least squares. In the calculations of f and of the mean velocity v, the minimum diameter of the pipe was used throughout, since it was felt that the corrugations might often contain pockets of "dead water" which do not contribute an effective part in the main pattern of flow.

C. M. Daniel (4) used the Weisbach-Darcy equation for frictional pressure loss and calculated friction coefficients for annular and helical type hoses. He indicates that the helical type hose has a lower pressure loss than the annular type. Very little worthy information was obtained from this paper.

R. C. Hawthorne (5) developed an analytical method for calculating pressure losses in corrugated hose and assumed that the corrugations behave as a series of uniformly spaced orifices. In this paper it was stated that corrugation height did not affect the flow (this is represented as ϵ in Figure 1). The empirical results were developed on this basis.

John Allen (6) found a critical Reynolds number of 1700 instead of the usual 2300. Also, the index of velocity was reported to be on the order of 2.4 at a Reynolds number of approximately 40,000 whereas for parallel piping the index does not exceed 2.0 after the transition region. This indicates a definite dependency on geometry.

Both Koch (7) and Nunner (8) in 1958 reported measurements of friction factors for flow tubes with artificial uniform roughness. Koch used orifice-shaped discs inside of a smooth pipe, and Nunner used rubber rings of semi-circular cross section. Both workers presented data which showed that friction factors were greater than those obtained for ordinary rough pipe. They also reported that there was a tendency for friction factors to increase in the neighborhood of Reynolds number equal to 10^5. Mobius (9) also performed work in this area. He used rings of square cross section and reported friction factors as high as 0.1.

In 1953 Wieghardt (10) conducted experiments involving flow over rectangular ribs placed at right angles to the flow. He also conducted studies of flow over circular cavities. Both of these systems gave an increase in the drag coefficient of the plate to which the ribs were attached or in which the holes were drilled. Photographs in the article show vortex patterns observed in the holes.

Wiederhold (11) and Seiferth and Kruger (12) report a water duct in which the mass flow rate decreased by 57% during a long period of usage. Both articles conclude that the increase in friction factor re-

resulted from a rib-like deposit of aluminum oxide on the walls of the duct. This rib-like geometry may be very similar to the geometry of the flexible hose used in the present study.

An article entitled "Boundary Layer Characteristics for Smooth and Rough Survaces" by F. R. Hama (14) presents an extensive bibliography in the area of flow over rough surfaces.

R. D. Mills (17) presents a two dimensional incompressible solution for the vortex motion of a fluid in a square cavity. Mills approached the problem from the standpoint of a periodic solution to the boundary layer equations. The result of his analysis is an infinite series expression for the velocity distribution in the cavity.

Results obtained from experiments on cross flow over cylinders may lead to a better understanding of the flow phenomena associated with flexible hose. Roshko (23) reported results for flow over cylinders in which the drag coefficient first decreases and then increases. This phenomena is due to boundary layer separation and motion of the separation point along the surface of the cylinder. A very large variation in the drag coefficient of the cylinder is produced by the motion of this separation point.

Clauser (25) reported data for flow in rough pipes. He stated that, "the customary zero velocity point is located at the variable height minus $\sqrt{2/c_F}$," where c_F is the locak skin friction coefficient. By adjusting the boundary condition in a manner such that the zero velocity occurs not at the wall, but at some point midway between the top of the protrusion and the bottom, he found that he could correlate the data more readily. A similar conclusion was made by Moore (16).

Knudsen and Katz (28) report the observation of eddy patterns in an area between fins on a transverse finned tube. They report that under almost all conditions of turbulent flow there is at least one eddy observed in the area between the fins.

Pepersack (29) prepared graphs to predict pressure losses in straight and curved sections of flexible hose. The pressure drops reported are from 4 to 19 times the loss through an equivalent smooth tube. A multiplying factor was recommended for predicting pressure loss. Results for a 90° bend, with R/D ranging from 6 to to 36 ft., are also presented in the form of a correction coefficient.

NOMENCLATURE

Symbol	Definition	Units
A	Area or constants (Equation 4, 17)	ft^2
β	Area or constants (Equation 4)	
D	Minimum hose diameter (inside)	ft
F	Force (Equation 17)	lb_f
f	Friction factor, Blasius	dimensionless
f_F	Friction factor, Fanning	dimensionless
f_o	Friction factor for zero bend angle	dimensionless
G	Mass flow rate	lb_m/sec. sq. ft
g_c	Conversion constant	$\frac{ft - lb_m}{lb_f\ sec.^2}$
h	Head loss (Equation 15)	$\frac{ft - lb_f}{lb_m}$
k	Constant (Equation 16)	
k_c	Depth of corrugation (Equation 14)	
L	Length of hose	ft
m	Mass	lb_m
P	Pressure	psi
ΔP	Pressure drop	psi
Re	Reynolds number	dimensionless
R_B	Bend Radius	ft
SCFM	Standard cubic feet per minute	ft^3/min
v	Velocity (Equation 9)	ft/sec.
w	Mass flow rate	lb_m/sec.

NOMENCLATURE (contd.)

Symbol	Definition	Units
α	Constant (Equation 1)	
β	Constant (Equation 2)	
σ	Geometric parameter (Figure 1)	ft
ϵ	Geometric parameter (Figure 1)	ft
λ	Geometric parameter (Figure 1)	ft
ρ	Fluid density	lb_m/ft^3
υ	Viscosity	$lb_m/ft\ sec.$

THEORETICAL CONSIDERATIONS

Definition of Friction Factor:

Consider the steady flow of a fluid in a conduit of uniform cross section. The fluid will exert a force F on the solid surface of the conduit. This force may be split into two parts: F_s, that force which would be exerted by the fluid even if it were stationary, and F_k, that additional force associated with the kinetic behavior of the fluid.

The magnitude of the force F_k may be arbitrarily expressed as the product of a characteristic area A, a characteristic kinetic energy per unit volume K, and a dimensionless quantity f, known as the friction factor:

$$F_k = AKf \qquad (17)$$

Note that f is not defined until A and K are specified. With this definition f can usually be given as a relatively simple function of the Reynolds number and the system shape.

In this study A is taken to be ΠDL, where D is the minimum inside diameter of the flexible hose, and K is taken to be the quantity $1/2\ \rho v^2$. Specifically, f is defined as

$$F_k = (\Pi DL)\left(\frac{1}{2gc}\rho v^2\right)f \qquad (18)$$

The quantity f defined in this manner is sometimes called the Fanning friction factor.

Momentum Balance:

According to Newton's second law, the rate of change of momentum equals the net applied force:

$$\frac{d(mv)}{dt} = \Sigma F \qquad (19)$$

The surface forces acting on an element of fluid in a pipe are due to the upstream pressure, the downstream pressure, and the peripheral shear. The momentum equation for a differential element of fluid is then

$$P \frac{\Pi D^2}{4} - (P + dP) \frac{\Pi D^2}{4} - \tau_0 \Pi D dx = v \frac{\Pi D^2}{4} \rho dv \qquad (20)$$

The peripheral shear stress can be expressed in terms of the friction factor f. From the definition of the friction factor

$$\frac{F_k}{A} = \tau_0 = Kf = \frac{\rho v^2}{2gc} f \qquad (21)$$

Inserting this relationship in the momentum equation and simplifying gives

$$\frac{dP}{\rho} + vdv + \frac{4fv^2 dx}{D2gc} = 0 \qquad (22)$$

This equation can then be integrated so as to give the working equation for the evaluation of the friction factor.

Friction Factor for the Water System:

For the flow of an incompressible fluid in a pipe of uniform cross section the integration of the momentum equation is straightforward.

$$dv = 0 \qquad \rho = \text{constant}$$

$$\therefore \frac{-\Delta P}{\rho} = 4f \frac{L}{D} \frac{v^2}{2gc} \qquad (23)$$

From this equation it follows that

$$f = \frac{1}{4} \left(\frac{D}{L}\right) \left(\frac{-\Delta P gc}{\frac{1}{2} \rho v^2}\right) \qquad (24)$$

This equation shows explicitly how f is calculated from experimental data.

Friction Factor for the Air System:

In order to integrate the momentum equation for a compressible fluid the variable density and velocity has to be expressed in terms of the variable pressure. It will be assumed that the system is operating under approximately isothermal conditions.

If all conditions are known at some upstream section, those at any arbitrary section downstream can be expressed in terms of known values at the upstream section. From the ideal gas equation of state,

$$\frac{P}{\rho} = \frac{P_1}{\rho_1} = RT = \text{constant}$$

From the equation of continuity,

$$v\rho = v_1\rho_1 = \text{constant}$$

$$\therefore \frac{dv}{v} = \frac{-dP}{P}$$

Inserting these relationships into the momentum equation and integrating gives:

$$\rho_1^{\,2} - \rho_2^{\,2} = \rho_1 v_1^{\,2} P_1 (4f\frac{L}{D} - 2\ln\frac{P_2}{P_1}) \qquad (25)$$

Introducing the Mach number $M = v/c$, the final working equation becomes

$$4\frac{fL}{D} = \frac{1}{kM_1^{\,2}}[1 - (\frac{P_2}{P_1})^2] - 2\ln\frac{P_1}{P_2}$$

$$f = \frac{1}{4}(\frac{D}{L})(\frac{1}{kM_1^{\,2}}[1 - (\frac{P_2}{P_1})^2] - 2\ln\frac{P_1}{P_2}) \qquad (26)$$

Variation of the Friction Factor:

The friction factor depends on a number of variables:

1. The geometry of the pipe
2. Reynolds number
3. The ratio L/D

Along the length of the pipe it is assumed that the geometry follows a regular pattern, therefore, this variable should cause no variation in the friction factor along the length of the pipe.

If the velocity profile is fully established at the entrance to the test section the friction factor will not depend on the ratio L/D. Only if the velocity profile is not fully established will this variable have to be considered.

This leaves only the investigation of the Reynolds number. Does the Reynolds number vary along the length of the pipe? For some cases it does, but for the great majority of cases it does not. Consider the case of an incompressible fluid flowing in a pipe of uniform cross section. Unless the fluid is heated, the density, viscosity, and diameter remain constant. The equation of continuity shows that the velocity also must remain constant, therefore, the Reynolds number must remain constant. It is obvious that the friction factor must remain constant along the length of the pipe.

For isothermal flow of compressible fluids the Reynolds number does not vary. If there are moderate changes in temperature the Reynolds number will not vary appreciably because the kinematic viscosity is not a strong function of temperature. For large changes in temperature the variation of friction factor along the length of the pipe should be taken into account in the analysis.

EQUIPMENT USED IN EXPERIMENTAL STUDY

The experimental apparatus used in this investigation was designed and constructed to yield data which had a good confidence level. Briefly, the equipment consists of two units. The first is designed to measure the rate of the flow of water through corrugated hose and the corresponding pressure losses; the second accomplishes the same objectives but with air as the flowing medium. Figures 2 and 3 are schematic diagrams of the experimental setup, and Figures 4 through 7 are photographs of the systems. Details of the equipment follow:

Water System:

1. Water was supplied by two centrifugal pumps connected in parallel. Each pump was powered by a U. S. Electrical, 3-phase, 220/440 volt, 7.5 h.p. electric motor and had the capacity to deliver 300 gpm with a 50 psig head. The water was stored in a rectangular tank and recirculated.

2. The flow rates were measured with two devices:

   a. A Builders Iron Foundry, Providence, R.I., 4.0 x 1.75 inch venturi meter for flow rates above 20 gpm; and

   b. A disc meter for flow rates below 20 gpm.

3. The flow rate was adjusted by manual setting of a 3" gate valve.

4. The pressure drop across the venturi meter was measured by a Builder-Providence, Inc. 22", single-arm, mercury manometer.

5. The pressure drop across the tests section was measured by

   a. Two "Bourdon" gauges for differentials above 15 psi

   b. A mercury w-tube manometer for differentials between 15 and 1 1/2 psi

   c. A CC14 w-tube manometer for differentials below 1 1/2 psi.

6. The temperature was measured by a 120° F mercury thermometer in a thermo-well.

Air System:

1. Air was supplied by

   a. One Davey Air Compressor rated at 210 CFM at 110 psi

   b. One Le Roi Air Compressor rated at 315 CFM at 125 psi

   c. A bank of electrically driven air compressors arranged in parallel to produce 250 CFM at 110 psi. The bank of compressors is located in the Mechanical Engineering Laboratories and were connected to this project in order to increase the overall capacity of the system.

2. The air-flow rate was measured with a standard orifice meter and mercury or carbon tetrachloride manometer.

3. The flow-rate was adjusted by use of a 3" Conoflow globe valve which was pneumatically actuated by a differential pressure ranging from 3 to 15 psi.

4. The inlet pressure to the hose was regulated and held constant by using a 2" Cash-Acme Pressure regulator, which had an operating pressure limit of 150 psi.

5. Pressure drops across the test sections were measured with standard type mercury or carbon tetrachloride differential manometers.

6. Pressure gauges and thermometers were installed in the system as indicated in Figure 3.

7. Pressure taps were located in the connection flanges of the test section. Damping valves were used in the connectors to minimize fluctuations of the manometer fluid level.

PRODUCTION OF DATA

Experimental Procedure:

The basic experimental procedure employed was as follows:

1. Water system

   a. Both pumps were started simultaneously and the system was allowed to stabilize.

   b. The high rates were tested first so the control valve was opened until a maximum reading was obtained on the manometer connected to the venturi meter.

   c. The pressure gauges on the test section were then observed to determine the range of pressure differential.

   d. If the range was above 7 1/2 psi, the readings of the gauges were recorded along with the venturi manometer reading. If the range was below this value the appropriate manometer (u-tube) lead valves were opened, the lines bled, and the differential recorded instead of the gauge readings.

   e. The flow rate was then decreased using the manometer across the venturi meter as a guide and the new flow meter and pressure differences were recorded.

   f. The procedure in step five was followed until a flow rate of approximately twenty gallons pèr minute was observed. The flow was then directed through the disc meter and all subsequent flow rates were obtained by using a stop watch to determine the time for 5 to 10 gal. to pass through the disc meter.

2. Air System

   a. Depending on the size hose being tested, one, two, or three of three available air compressors were started and the line pressure was allowed to reach 125 lbs. of pressure.

   b. The first reading on any given hose was taken at a pressure of 40 psig (if achievable) on the inlet to the test section. The hose was initially at zero degree bend angle.

   c. The flow rate was then varied until a predetermined pressure drop (across the test section) was approximated. The exact pressure drop was measured with a differential manometer.

d. This reading was then recorded along with the inlet temperature and pressure on the orifice section, and the pressure drop across the orifice.

   The pressure drops were measured with manometers and the other pressures with a gauge. Both temperatures were measured with Fahrenheit thermometers.

e. The flow rate was then increased, the inlet pressure being held constant, until the second predetermined pressure drop had been reached.

f. All readings were recorded. This procedure was repeated for all other pressure drop settings.

g. Steps 1 through 6 were then repeated for all other bend angles being tested.

Range of Measurements:

Experimental measurements of flow rate, pressure drop, and temperature were carried out over a range of conditions. For the water experiment the ranges recorded were:

flow rate - <1 gpm to 300 gpm

Reynolds number - 6000 - 380,000

ΔP across test section - 3.5 psi/ft. to 0.01 psi/ft.

Temperature - $40^\circ F \rightarrow 80^\circ F$

For the air system:

Inlet pressure - $20 \rightarrow 50$ psig

Pressure drop ratio $(\frac{\Delta P}{P})$ $10^{-3} \rightarrow 0.5$

Temperature $50^\circ F \rightarrow 120^\circ F$

Reynolds number $10^4 \rightarrow 5.5(10)^5$

SCFM $5 \rightarrow 1100$

The temperatures for the water system varied with the season, whereas for the air system a combination of season and compressor effects caused the temperature to change.

CALCULATIONS AND COMPUTER TECHNIQUES

The computer programs developed for this study can be divided into two categories:

1. Data reduction and correlation
2. Prediction

The data reduction programs have been presented in a previous report. They will also be given in volume 3 of the final report. Basically, these programs perform the same series of calculations. Data taken on the test system is coded and read into the computer. The programs convert this data into quantities such as flow rates, pressure drop, Reynolds number, friction factor, etc., which can then be used for analysis and correlation.

The correlation programs were basic regression programs. Most of these programs were available from the LSU computer center and, hence, will not be given in this report. Those programs written especially for this project are presented in volume 3.

The final programs developed for predicting friction factors are written in Fortran IV. These are presented in volume 3 along with instructions for input and operation.

EXPERIMENTAL RESULTS

Water System:

1. Pressure drop

Pressure losses across the test section were measured under the experimental conditions shown previously. These measurements were made using: (1) pressure gauges for measured differentials of 15 psi and greater, (2) a mercury-filled, U-tube manometer for differentials in the range of 15 psi down to 1.5 psi, and (3) a carbon tetrachloride filled, U-tube manometer for measured differentials below 1.5 psi. The observed pressure losses across the test sections ranged from 35 psi down to 3 inches of carbon tetrachloride. The actual observed magnitude of the pressure loss range was dependent on the size of the pipe and the flow rate.

The accuracy of the pressure loss measurements had several limitations:

a. The gauges, even though they were dampened considerably, had noticeable fluctuations at high flow rates due partially to the extremely turbulent nature of the flow and partially to the head fluctuations of the pumps in these ranges.

b. When the flow rate was decreased steadily during a run there existed the possibility of hysteresis in the gauges.

c. Even though care was taken to fully bleed the manometer lead lines, the observed differentials of less than 40 inches of CC_4 (corresponding to pressure losses of less than 0.1 psi per foot of hose) many times gave a continuous error which gave the appearance of a "tailing effect" on the lower end of the pressure drop vs. Reynolds number curve as illustrated below by the dashed line in Figure[8]. It should be noted that this effect was noticed at Reynolds numbers in excess of the laminar-turbulent transition range for smooth pipes.

d. The flexible hose themselves contributed to error in the data in that due to their inherent expansion and contraction with changes of exit pressure additional pressure loss could be observed if a slight kink in the hose were to occur. This effect was artifically produced several times and found to be slight but not entirely negligible.

2. Pressure drop across the venturi meter

All flow rates above 20 gpm were measured as a logarithmic function of the pressure reading across a 4.0" x 1.75" throat venturi meter. This pressure difference was measured by a single arm, mercury-filled manometer of 22 inches maximum differential.

There were two main limitations on the accuracy of the pressure loss across the venturi:

a. The head fluctuations of the pumps in certain ranges caused the manometer to fluctuate slightly. This was normally in the order of plus or minus one or two tenths of an inch, which in the range in which it occurred meant less than 3% error in the calculated flow rate.

b. The manometer scale was divided into tenths of an inch; and, while no noticeable fluctuations occurred at readings below 0.5 inches, the readings in this range were limited by the accuracy of interpolation between 0.1 and 0.2 inches (19 to 27 gpm) and so on, such that calculated flow rates in this range could have been as much as 10% off.

3. Timing the disc meter readings

The flow rates below twenty gallons per minute were measured by timing the movement of the indicator around the 10 gallon dial (graduated in gallons) of a standard disc meter. Calibration of this meter showed it to be within 2% of the true value until a flow rate of less than 2 gpm was reached. At 1 gpm (the lowest used in testing) the accuracy was found to be within 5%.

The only other inaccuracy in using the disc meter was the difficulty in reading exactly 10 gallons on the clock type dial. This was a problem only in the range of 15 to 20 gpm (45 to 30 sec. on the stop watch) and this was less than ±.1 of a gallon, or 2%.

Air System:

1. Accuracy of data

a. Pressure drop across the test section - Pressure drops were measured under the experimental conditions discussed previously. At a given inlet condition - i.e., known inlet pressure and temperature - the pressure drop increased with an increase in flow rate. Figure (9) shows this effect for the 1 1/2 inch diameter closed pitch hose which is considered as the model for all tests. The data shown are for a zero bend angle condition.

The accuracy of the pressure drop measurements is determined by several factors:

1. Uncertainties in the manometer readings. These could be caused by human error, manometer fluid fluctuations, slight variations in flow rate due to changing thermodynamic conditions, and at very low velocities the limitations of the instruments used.

2. Flow disturbance effects. The fact that the manometer leads were attached to the connecting flanges, which by necessity were located between two sections of corrugated hose, could affect the readings.

   The main stream leaves a rough or corrugated section, enters the relatively smooth section of the flange, and then re-enters a corrugated section. The loss in precision due to this transition is not known.

3. Turbulence effects. The fluctuating velocity components associated with turbulent flow could affect the manometer readings. Since the intensity of turbulence is unknown in this system this effect cannot be evaluated.

4. Reynolds number effects. At very low Reynolds numbers (based on the minimum hose diameter) the velocity is very low and there is a loss of precision in the pressure measurements.

b. Pressure drop across the orifice - The pressure drop across the orifice is used to calculate the flow rate of air through the system under a given set of inlet conditions.

The accuracy of these measurements are also limited by several factors:

1. The uncertainties in manometer readings are due to the reasons cited above.

2. High velocity effects. If the velocity is high enough so that Mach 1 is reached at the orifice, then the pressure drop readings are erroneous. This will alter the calculated flow rate and in turn the final results will be misleading.

c. Other pressure measurements - Pressure measurements were made at the location indicated in Figure 3. The accuracy of these measurements depended a great deal on the accuracy of the gages. Calibration curves were determined for each gage as often as it was deemed necessary. The probable variation in pressure readings from the gages was 2 or 3 percent at the lowest readings (20 psi).

The pressure of the inlet of the test section was used in calculating the inlet Mach number, and in the determination of the pressure at the exit of the test section.

The pressure readings from the gages on the downstream side of the orifice were used only as an indication of the pressure drop across the orifice. The pressure on the upstream side of the orifice was used in flow rate calculations.

An additional uncertainty in the pressure readings arises from hysteresis effects in the gages.

d. Temperature measurements - Temperatures recorded at the inlet section were used in calculating inlet Mach numbers. The temperatures across the orifice were used in flow rate calculations.

The most critical point in the system with respect to temperature measurements appeared to be at the test section inlet. Here, the effect of compressor heating was very noticeable and the rise in temperature during one test run could be as much as 5°F. Other than this effect of the compressors there were no other reasons for the temperatures to be questionable.

2. Special Treatment of Data for the Air System

a. Reduced pressure data - The pressure drop data shown in Figure (9) was reduced to a common curve by plotting

$\Delta P/P_1$ versus $W\sqrt{T_1}/P_1$. The result for the 1 1/2 inch closed pitch hose (zero bend angle) is shown in Figure (10). In the range of $\Delta P/P_1$ from 0 to approximately 0.1 the data shows a straight line variation. Above $\Delta P/P_1$ of approximately 0.1 the slope increases and $W\sqrt{T_1}/P_1$ tends to attain a limiting value. The reason for this increase in slope is unexplained, as is the value of $\Delta P/P_1$ at which it occurs. One possible explanation is in the effect of hose geometry. If there occurs in the length of hose tested a transition from one type of flow - i.e. fully turbulent and unaffected by geometry - to a flow pattern totally dependent on geometry, then there could occur a marked change in pressure drop. This, in effect, says that a new energy function is present and the evaluation of terms in the energy balances by use of the correlations and methods described for conventional isothermal or adiabatic flow is not satisfactory for the actual process. The generation of a vortex motion within the convolution and the resultant increase in boundary layer effect would be one instance of this.

The exact mechanism will remain unexplained until further work is done in defining the actual velocity profile, turbulent intensity and other flow parameters.

The curves of $\Delta P/P_1$ versus $W\sqrt{T_1}/P_1$ were to be used in friction factor calculations. Although a suitable equation was found to describe the curve, it was dependent on inlet pressure and the $\Delta P/P_1$ value at which the increase in slope began. Attempts to define this point exactly were unsuccessful. In addition, it was decided that data reduction techniques would only have meaning for the system in question and would not be general enough for NASA's use.

b. Friction factors - Friction factors were determined from pressure drop measurements by use of equation (26). As a result, the final plots of friction factor versus Reynolds number represent point data and show considerable scatter. The number of values determined was limited by the capacity of the experimental equipment.

The calculated values of friction factor found in this way are tabulated in Volume II of this report. Figure (11) shows the general trend of data and is taken as a representation of friction factor effects for all hose tested. It is again evident from Figure(11) that the hose geometry affects the friction factor. Further, the changes in momentum and thermodynamic parameters for a length of hose in conjunction with hose geometry becomes a significant variable in reducing data. The values of friction factor presented are interpreted to be average values calculated from data representing overall changes in a set length of hose.

In order to show the friction factor as one curve, as it is for standard pipe, a plot was made of friction factor versus $W\sqrt{T_1}/P_1$. The results are shown in Figure (12). Again, this type of correlation would have little meaning in a general design calculation since the inlet pressure is a variable.

DISCUSSION OF RESULTS

Water System:

1. Correlation for Straight Hose

The friction factor for the water system was correlated as a function of Reynolds number and hose geometry. For a straight hose the mathematical equation has the form:

$$f_F = \alpha Re^{\beta} \tag{27}$$

where α and β are functions of geometry. Note that this equation has the same functional form as the well-known Blasius formula for turbulent flow in a smooth tube:

$$f = 0.0791\ Re^{-2.5} \tag{28}$$

If equation 27 is plotted on log-log paper it will be seen that a straight line results. In regard to this straight line the term β is the slope and the term α is the intercept. These terms, slope and intercept, will be used interchangeably with β and α.

In order to discuss the exact functional forms of α and β the geometry of flexible hoses must be classified. A common system of classification has been as follows:

- I. Annular
  - A. Close Pitch
  - B. Open Pitch
- II. Helical

For the purposes of this study it was found that annular type hose need not be broken down into open or close pitch. The correlations developed in this study were found to be applicable to both types considered as just annular hose.

As mentioned above, the term α is a function of hose geometry. It was found that two correlations were needed to define this function - one for annular type hose and one for helical type hose. The functional form of the relationship for annular type hose is as follows:

$$\alpha = 0.01588\left(\frac{\lambda - \sigma}{\epsilon}\right) - 0.00215 \tag{29}$$

This equation is shown plotted with the observed data points in Figure (13) of the appendix. The correlation coefficient for this equation was 0.976. For 14 degrees of freedom this value means that correlation is significant at the 99.9% confidence level. The F value calculated for this correlation was 650. This F value of 650 is far beyond the range of reasonable chance variation.

The correlation for the helical-type hose is similar:

$$\alpha = 0.02916\left(\frac{\lambda - \sigma}{\epsilon}\right) - 0.00886 \tag{30}$$

The correlation coefficient for this equation was 0.975. For 6 degrees of freedom this correlation is also significant at the 99.9% confidence level. The F value determined for this equation was 2295.

The term β was found to be a function of the geometric parameter $(\sigma\epsilon/\lambda^2)$. The correlation developed with this parameter is independent of the type of hose used - that is, it can be used for both helical and annular type hose. The functional form of this correlation is:

$$\beta = 0.2987\left(\frac{\sigma\epsilon}{\lambda^2}\right) - 0.0313 \tag{31}$$

The correlation coefficient calculated for this equation was 0.848. For 22 degrees of freedom this correlation is significant at the 99.9% confidence level. The F value was 112. This equation is shown plotted in Figure (15) of the appendix. The observed data points are also shown on this graph.

Using the preceding correlations the friction factor for a straight hose can be predicted at a given Reynolds number. In order to do this, it is first necessary that the hose geometry be known. Once the geometric parameters are set for a given hose the values of α and β for that hose can be determined. The relationship between friction factor and Reynolds number is thus defined.

2. Correlation for Curved Hose

The correlation for bend angles other than 0^{o} has been found to be independent of the type of hose used. For both annular and helical type hose the correlation is:

$$\frac{f}{f_o} = 1.0 + 7.898 \left(\frac{D}{R_B}\right)^{0.896} \tag{32}$$

The correlation coefficient was determined to be 0.773. For 142 degrees of freedom this correlation is significant at the 99.9% confidence level.

Note that f_o is the friction factor determined at a bend angle of 0^{o} (straight hose). This value can be determined either by experiment or from correlations.

As the correlation given in equation 32 indicates, the ratio of f/f_o is independent of Reynolds number. Schlickting (4th edition, p. 530) states that C. M. White has found that the resistance coefficient for turbulent flow in a curved pipe can be represented by the equation:

$$\frac{f}{f_o} = 1.0 + 0.075\, Re^{1/4} \left(\frac{r}{R_B}\right)^{1/2} \tag{33}$$

where r is the radius of the cross section and R_B is the radius of curvature. Note that this equation has the Reynolds number stated explicitly as a variable. For flexible hose the Reynolds number does not appear to be a significant variable.

3. Accuracy of Correlations

Table 2 gives an indication of the accuracy of the correlations developed for the water system. For each hose and bend angle the average error (%) and average standard deviation (%) are given. These quantities are calculated from observed and predicted friction factors.

4. Limitations of Correlations

These correlations were developed from data which extended over a Reynolds number range of from 6,000 to 380,000. The reliability of the correlations for Reynolds numbers below 6000 is doubtful. However, it appears reasonable to use these correlations at Reynolds numbers moderately above 380,000. Below 6000 the problem of transition from turbulent to laminar flow becomes critical - especially at large values of curvature.

The bend angle correlation was developed from data covering a range of D/R_B from 0 to 0.0787. This corresponds to a variation in the bend radius of from 3.18 ft. to infinity (straight hose).

5. Effect of Reynolds Number

The following data shows the effect of Reynolds number on friction factor for a 1 1/4 inch open pitch hose at 0^{o} bend angle.

Reynolds Number	Friction Factor
10,700	.01757
12,900	.02034
14,500	.01665
17,800	.01926
20,800	.01773
26,300	.01546
32,900	.01813
40,800	.01750
54,500	.02166
62,000	.02204
69,300	.01958
75,900	.02032

Reynolds Number	Friction Factor
87,600	.02108
97,900	.02175
111,600	.02133
123,800	.02298
138,400	.02403
157,700	.02347
169,400	.02280
180,300	.02303
195,500	.02390

It appears from the data that the friction factor increases steadily with increasing Reynolds number. Note that although the pipe wall is very rough and the flow is completely turbulent the friction factor is not constant.

An interesting experimental oddity is observed because of the result stated above. If the viscosity of the fluid flowing in the flexible hose is increased, the pressure drop observed will decrease. This is because the Reynolds number is inversely proportioned to the viscosity - a decrease in viscosity will cause an increase in Reynolds number and hence, an increase in the friction factor. This, in turn, results in an increase in pressure drop for the same fluid velocity.

Consider the effects of a change in temperature on the water system. The density of water is not a strong function of temperature, hence there will be very little change in velocity. The viscosity of water, however, is a strong function of temperature - a 30°F change causes a 34% change in viscosity. This means that an increase in temperature of the water would decrease the viscosity without greatly affecting the density. The increase in Reynolds number could be as much as 30% and this would cause an appreciable increase in the friction factor. Pressure drop would be expected to increase.

This effect probably stems from the fact that circulating eddies are present in the hose convolutions and causes the mechanical energy to be degraded at a greater rate than commonly experienced in normal pipe. This is indicated by the fact that β has been observed to be greater than zero, showing that the friction factor is not constant.

Air System:

1. Correlation for straight hose

The friction factor for the air system was correlated as a function of Reynolds number and hose geometry. For a straight hose the mathematical equation has the same form as the equation used in the water correlation, namely:

$$f_F = \alpha Re^{\beta} \tag{27}$$

Where α and β are again functions of geometry. The functional form is the same as before with only the basic relationships for α differing from those found in the water system. For annular type hose the relationship for α is:

$$\alpha = 0.02202\left(\frac{\lambda - \sigma}{\epsilon}\right) - 0.00287 \tag{34}$$

The correlation coefficient for this equation is 0.987. For 14 degrees of freedom this value means that the correlation is significant at the 99.9% confidence level. The F value calculated for this value was 1019. For the helical type hose α is given by:

$$\alpha = 0.04306\left(\frac{\lambda - \sigma}{\epsilon}\right) - 0.01318 \tag{35}$$

The correlation coefficient for this equation is 0.904, the degrees of freedom are and F is 534. As stated previously, β has the same functional form that was found for the water system and the correlation coefficients are the same.

Although the above correlation adequately predicts the friction factor at a given Reynolds number for a straight hose, there is a definite limit in the range of Reynolds numbers where this equation is satisfactory. The basic data indicates a dependency of friction factor on thermodynamic properties and momentum parameters. By considering the limited amount of information available with respect to changes in flow variables along the hose, a conclusion was reached regarding the factors limiting the above equation. At a velocity in the neighborhood of 140 ft./sec., the friction factor increased at a greater rate than the correlation would predict. Figure (11) clearly shows this phenomena as a function of inlet pressure. If adequate data on the flow mechanism present in the hose and on the thermodynamic variable involved were available, then, a definite conclusion concerning this transition could be made.

Correlation equations were not developed for the friction factors above the transition point. As a result, the correlations presented are only good in the range of Reynolds numbers below the transition point. This, in effect, says that velocity is a significant variable.

2. Correlation for curved hose

The correlation for bend angles other than 0° has been found to be of the type of hose used. For both the annular and helical type hose the correlation is the same as that found for water, namely:

$$\frac{f}{f_0} = 1.0 + 7.898\left(\frac{D}{R_D}\right)^{0.896} \qquad (32)$$

The correlation coefficients and other considerations are also the same as those found for the water system and are not repeated here.

3. Accuracy of bend angle correlation

Table III gives an indication of the accuracy of the correlations developed for the bend angles on the air system. Note that the values shown are below the transition Reynolds number and only refer to the straight line portion defined by the correlation equations.

4. Limitations of correlations

The correlations were developed from data which extended over a Reynolds number range from 14,000 to 580,000. The reliability of the correlations for low Reynolds numbers are questionable due to the over-all scarcity of data in these ranges. The scatter over the entire range of Reynolds numbers is primarily due to the instrumentation used and the problem which was to be solved. The two were not compatible and it is felt that a new and sophisticated approach to the instrumentation problem is needed.

The correlations are also inadequate for a main stream velocity range above approximately 140 ft./sec. The Reynolds number at which this velocity occurs is a variable depending on the diameter of hose.

Although there is a question of validity at the low Reynolds numbers, it appears reasonable to accept the correlations in estimating design criteria.

The bend angle correlation was developed from data covering a range of D/R_B from 0 to 0.0787. This corresponds to a variation in the bend radius of from 3.18 ft. to infinity (straight hose.)

CONCLUSIONS

The following conclusions can be made concerning the study of flow losses in flexible hose:

Water system

1. An empirical method has been developed for predicting the Fanning friction factor for the flow of an incompressible fluid in a flexible hose.

2. The correlations developed indicate that the friction factor is a function of two dimensionless geometric parameters and Reynolds number.

   a. The bend angle correlation also is a function of the geometric ratio D/R_B.

3. The friction factor is not constant at large values of the Reynolds number. This study has shown that generally the friction factor increases with increasing Reynolds number.

4. For flow in flexible hose, mechanical energy is degraded at a rate 4 to 5 times faster than for flow in a smooth tube of the same size and at the same velocity.

5. The empirical correlation developed in this study can predict friction factors with an accuracy in the order of $\pm$ 20%.

Air system

1. Friction factors for the air system average 20-25% higher than these obtained for the water system for the same hose and at the same Reynolds number.

2. An empirical method was developed to predict friction factors over a limited range of Reynolds numbers.

   a. The correlation is reliable up to a linear velocity of approximately 140 ft./sec. Above this value, the friction factor increases at a rate greater than the empirical correlation predicts.

   b. Above 140 ft./sec. other variables, not included in the present correlation, must be taken into account.

3. Because of problems in flow control and measurement, the test system for air was not reliable for studying flow behavior above a velocity of 140 ft. /sec.

4. Further work must be done on the air system in order to obtain an understanding of the high velocity region. Specific recommendations have been made in other parts of this report.

RECOMMENDATIONS

As pointed out in the Discussion section, the present study has developed an empirical equation which can be used to predict the pressure drop that will result from the flow of any gas or Newtonian liquid through a flexible hose of known dimensions.

The utility of, and the confidence in the correlating equation can be improved by further investigation with these specific objectives.

1. To develop a better understanding of the flow mechanisms and phenomena which are responsible for the differences in the behavior of friction factors in flexible, corrugated hose and those in smooth, rigid pipe: for example, their positive variation with Reynolds number for both liquids and gases. This behavior, found in the present study, was noted in many of the literature references cited in this report; qualitative explanations of it have been given in the discussion section, but study is needed to verify and quantify these.

2. To study the region of relatively high velocity gas flow in which it was observed that there was systematic deviation from the basic linear friction factor-Reynolds number plot. This was most evident in the smaller sizes of open pitch hose. Additional data are needed to ascertain the influence of pressure, pipe length, or other responsible parameters and to test the causes postulated for it. Study of these pipes with or near sonic flow limitations would be informative if these flows can be attained.

3. To obtain better and statistically sounder constants α and β, as defined and correlated in Equations (1) and (2) for use in predicting the friction factor for any hose. These equations utilize the three geometric dimensions which describe flexible hose - pitch, depth, and width of the corrugations. The range of variation, and the number of

points used in deriving these was limited: now that the significant variables have been identified, selection and test of a few additional hose, and the incorporation of the results in new equations (1) and (2) should extend their validity considerably.

To accomplish this objective, it is proposed that the basic approach be modified to investigate fundamental quantities which the work just concluded has indicated is most needed. For example, studies of the velocity profiles in the main stream of the tubes (i.e., the center core) and of the flow patterns in the annular or helical segments created by the corrugations would contribute greatly to the understanding of the pressure drop behavior. If the various mechanisms that consume mechanical energy as "friction" can be isolated and evaluated separately, the results would be of immeasurable value in predicting the pressure drop or - at the very least - in guiding and interpreting empirical correlations. Realization of this objective would require the use of hot wire anemometers or the ingenuous application of other techniques for measuring point velocities. These studies would be made on the available hose sections; a few new ones could be added to obtain a wide range of shape factors, as suggested above.

A related but independent extension of this study would be to the simultaneous flow of gas and liquid through these flexible hose. The influence of the corrugations on the flow patterns - i.e., the probability that the liquid would collect in and fill the corrugations suggests that it would decrease the area available for flow and thereby increase the pressure drop; the extent to which this effect would occur would depend on the pipe orientation (horizontal or vertical). It can be established only by experimentation. This study would build upon the experience acquired in handling the two fluids separately; the apparatus would require a moderate amount of modification.

APPENDIX I

REFERENCES

1. A. H. Gibson. Flow of water in a corrugated pipe. Phil. Mag., Vol. 50, ser. 6, 1925, pp. 199-204.

2. M. J. Webster and L. R. Metcalf. Friction factors for corrugated metal pipes. Proc. Amer. Soc. Civ. Engrs., Vol. 85, No. HY9, September, 1959, pp. 35-67.

3. C. R. Neill. Hydraulic roughness of corrugated pipes. Proc. Amer. Soc. Civ. Engrs., Vol. 88, No. HY3, May, 1962, pt. 1, pp. 23-44.

4. C. M. Daniels. Pressure losses in flexible metal tubing. Product Engineering, April, 1956, pp. 223-227.

5. R. C. Hawthorne. Flow in corrugated hose. Product Engineering, June, 1963, pp. 98-100.

6. John Allen. Flow of incompressible fluids through corrugated pipes. The Institute of Civil Engineers, Vol. 28, May, 1964, pp. 31-38.

7. R. Koch. Pressure drop and heat transfer for flow through empty, baffled, and packed tubes. VDI Forschungsheft 469, 1958.

8. W. Nunner. Heat transfer and pressure drop in rough pipes. VDI Forschungsheft 455, 1958.

9. v. H. Mobius. Experimentelle Untersuchung des Widerstandes und der Geschwindigkeitsverteilung in Rohren mit regelmässig angeordneten Rauhigkeiten bei turbulenter Strömung. Physik Zeitschrift 41:202-225, 1940.

10. K. Wieghardt. Erhöhung Des Turbulenten Reibungswiderstandes Durch Oberflachenstorungen. Forschungshefte Für Schiffstechnik 1. 65-81, 1953.

11. v. W. Wiederhold. Uber den Einfluss von Rohrablasgerungen auf den Hydraulischen Druckabfall. Gas - und Wasserfach 90:634-341, 1949.

12. R. Seiferth and W. Krüger. Überraschend hohe Reibungsziffer einer Fernwasserleitung. Zeitschrift V. D. I. 92:189-191, 1950.

13. J. Doenecke. Contribution À L'Étude de la Convection Forcée Turbulent le Long de Plaques Rugueuses. International Journal of Heat and Mass Transfer 7:133-142, 1964.

14. F. R. Hama. Boundary-layer characteristics for smooth and rough surfaces. Soc. of Naval Arch. and Marine Engrs. 62, 333-358, 1954.

15. W. D. Baines. An exploratory investigation of boundary-layer development on smooth and rough surfaces. Ph. D. dissertation, State University of Iowa, 1950.

16. W. F. Moore. An experimental investigation of the boundary-layer development along a rough surface. Ph. D. dissertation, State University of Iowa, 1951.

17. R. D. Mills. On the closed motion of a fluid in a square cavity. Journal Royal Aero. Soc. 69, 116-120, 1965.

18. W. W. Baturin. Lüftungsanlagen für Industriebauten. 2nd ed., Veb Verlag Technik, Berlin, 1959, p. 187.

19. A. Roshko. Some measurements of flow in a rectangular cut-out. NACA TN 3488, 1955.

20. R. D. Mills. Flow in rectangular cavities. Ph. D. thesis, London University, 1961.

21. W. Linke. Stromungsvorgänge in Zwangsbelufteten Raumen. VDI Berichte 21, 1957.

22. V. K. Migay. The aerodynamic effectiveness of a discontinuous surface. Inzhenerno-Fizicheskiy Zhurnal, 5, 20-24, (AD602564), 1962.

23. A. Roshko. Experiments on the flow past a circular cylinder at very high Reynolds number. Journal of Fluid Mechanics, 10, 345-356, 1961.

24. S. Corrsin and A. Kistler. The free-stream boundaries of turbulent flows. NACA TN 3133, 1954.

25. F. H. Clauser. Turbulent boundary layers in adverse pressure gradients. Journal Aero. Sci. 21, 91, 1954.

26. J. Laufer. The structure of turbulence in fully developed pipe flow. NACA Tr 1174, 1954.

27. J. O. Hinze. Turbulence. McGraw-Hill, New York, 1959.

28. J. G. Knudsen and D. L. Katz. Fluid Dynamics and Heat Transfer. McGraw-Hill Book Co., Inc., New York, 1958, pp. 192-197.

29. F. J. Pepersack. Pressure losses in flexible metal hose utilized in propulsion fluid systems of XSM-68B and SM-68B. Technical Memorandum, Baltimore, Martin-Baltimore, September 1960, pp. 25-40

APPENDIX II

FIGURES AND TABLES

Figure 2

SCHEMATIC DIAGRAM

AIR OPERATION

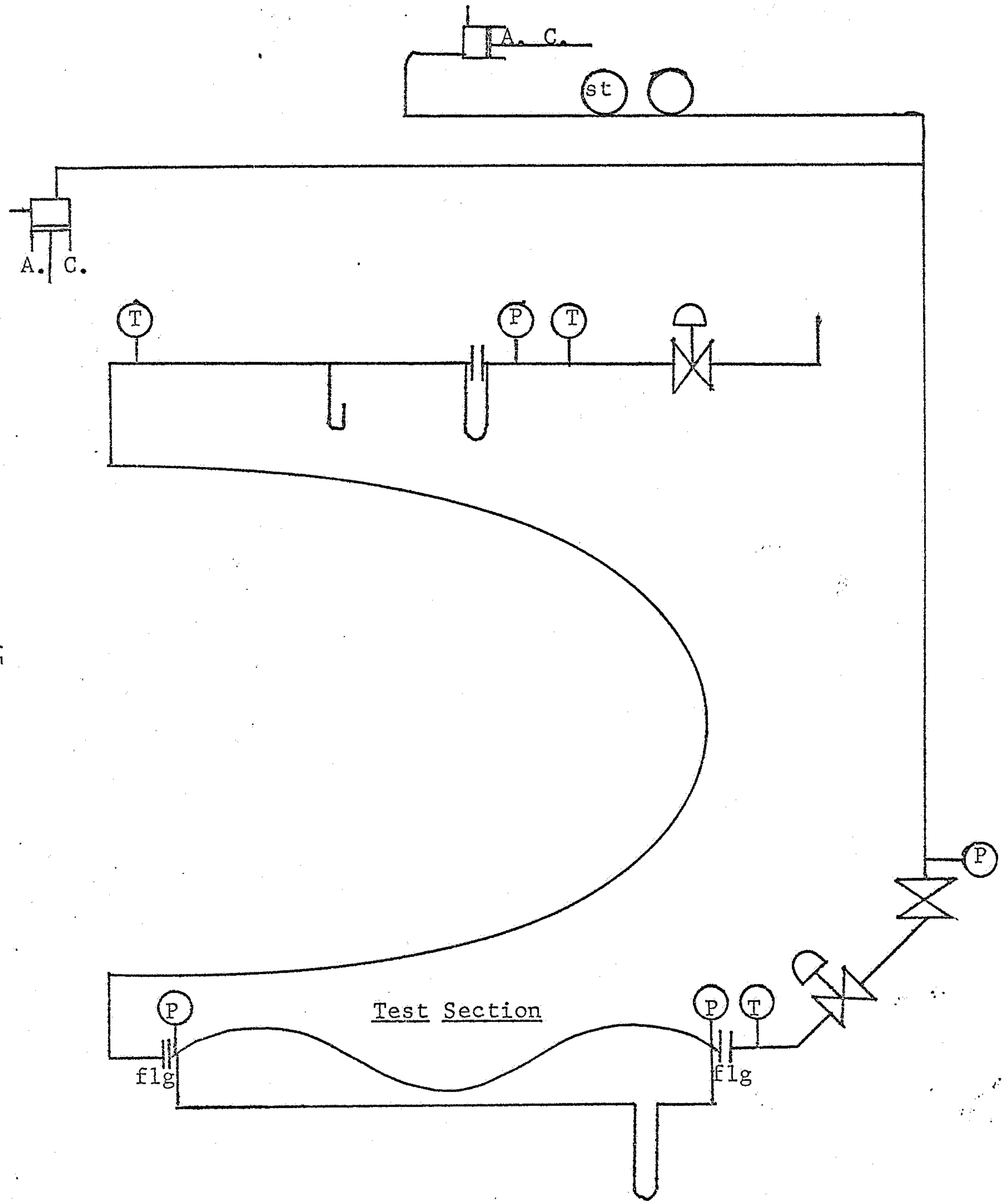

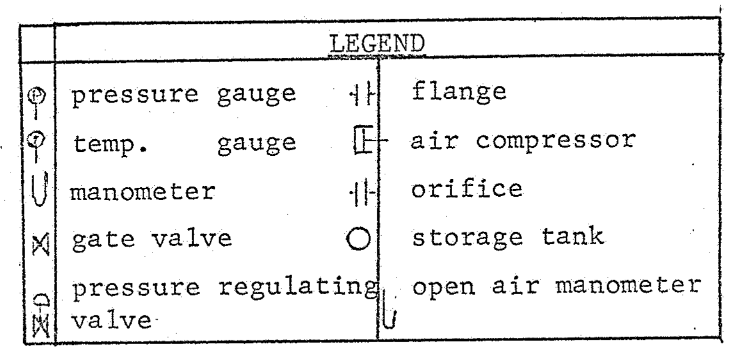

Figure 3

SCHEMATIC DIAGRAM

WATER OPERATION

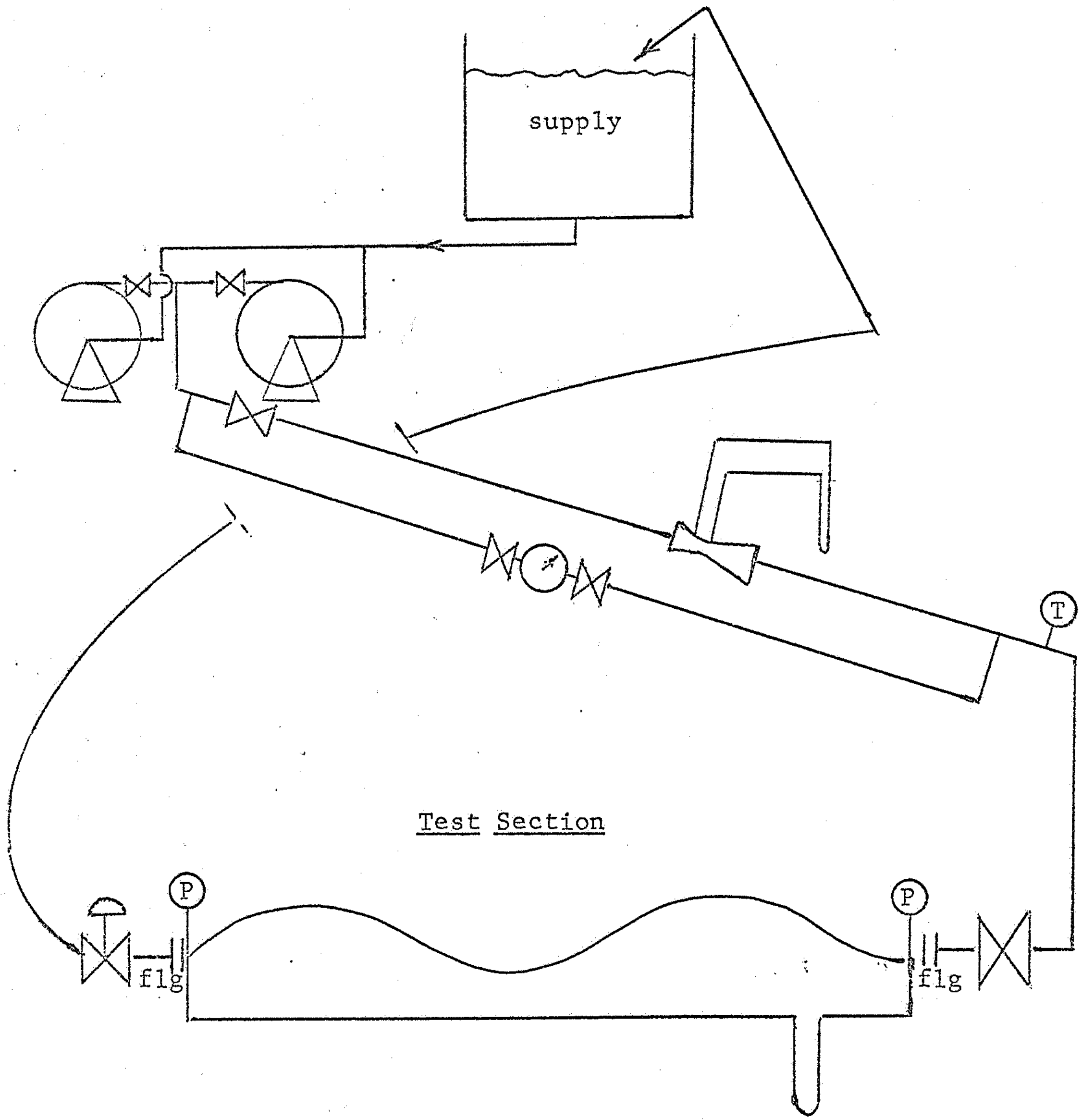

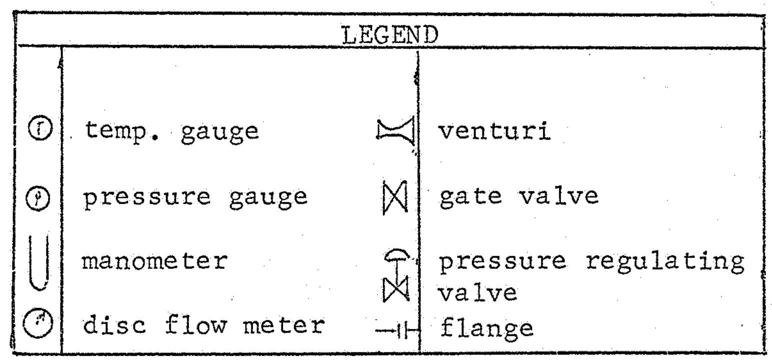

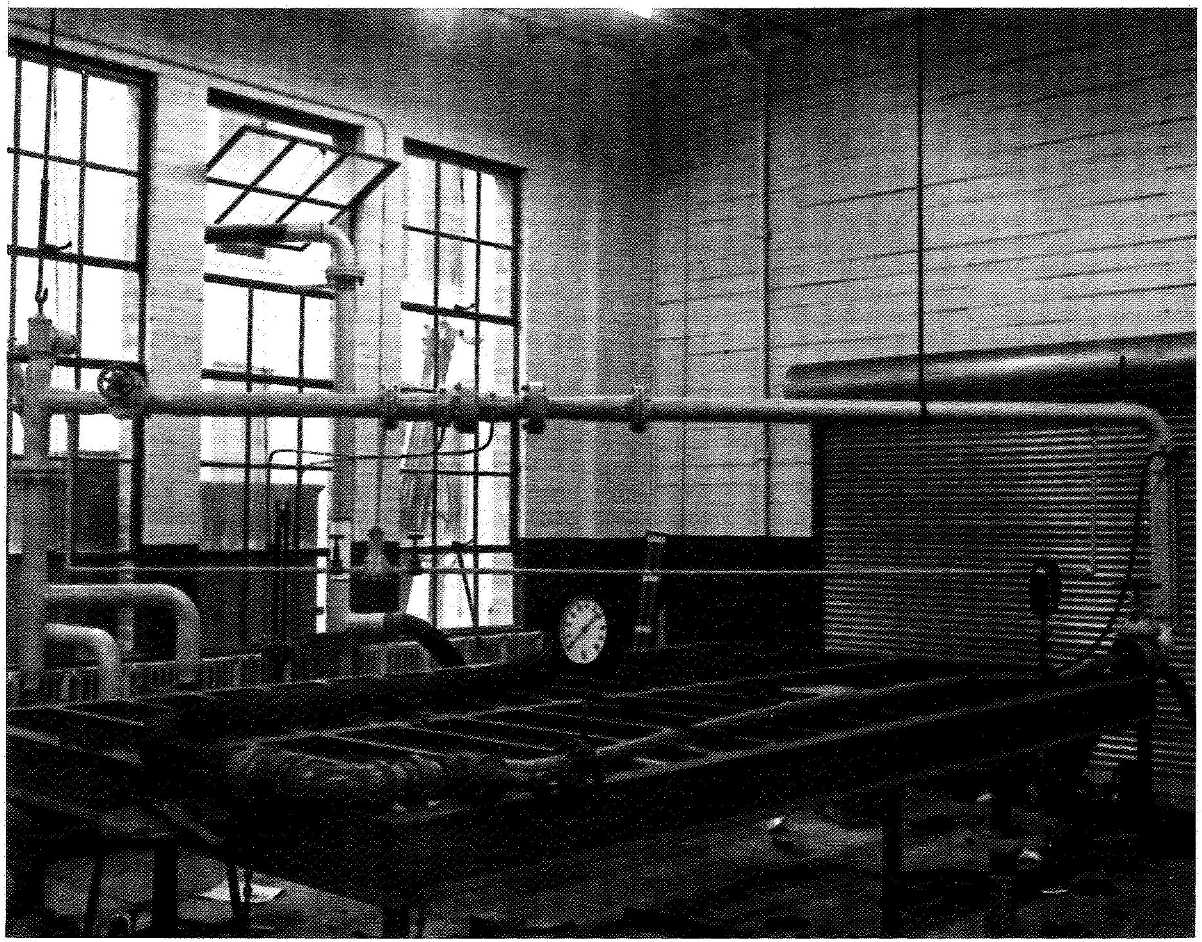

DATA PRODUCTION SYSTEM FOR WATER FIGURE 4.

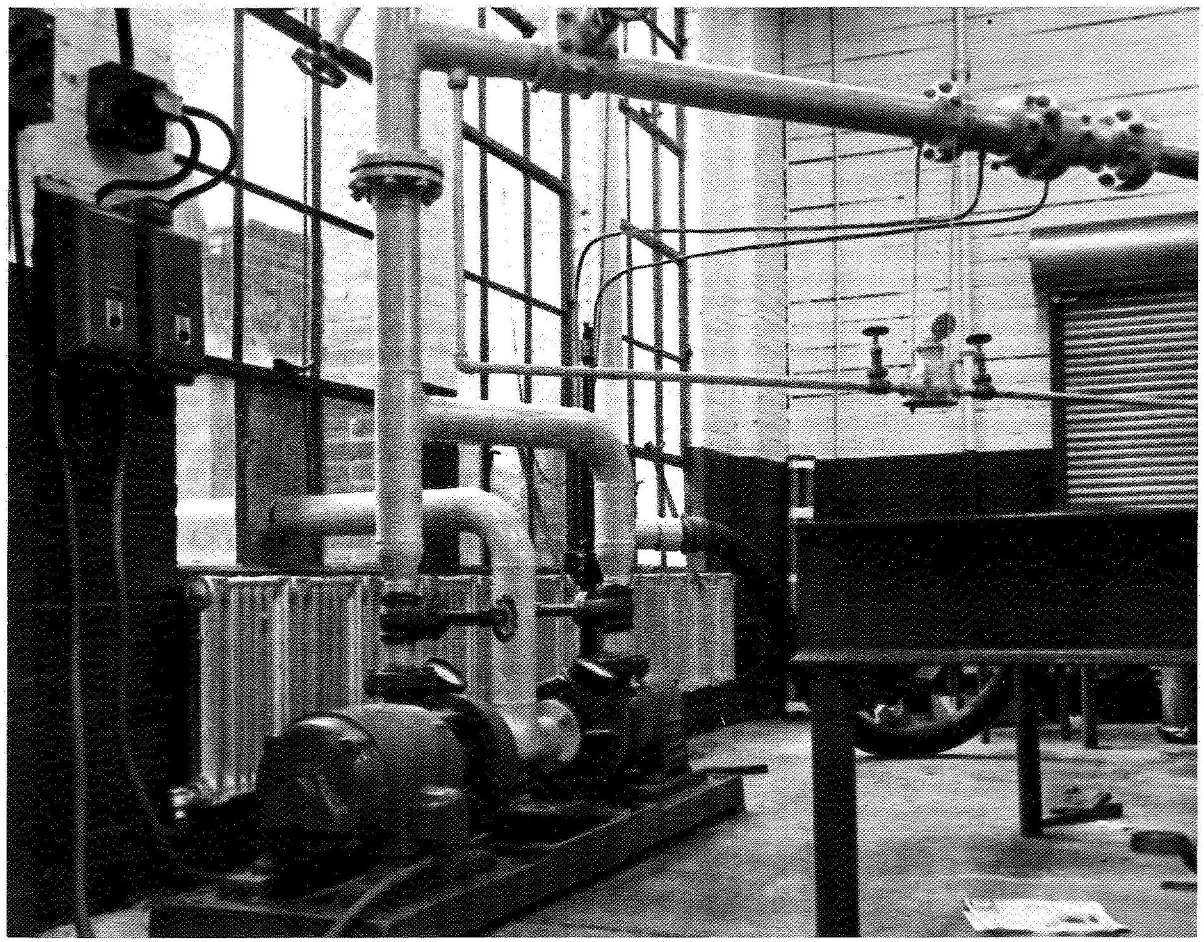

DATA PRODUCTION SYSTEM FOR WATER
SHOWING PUMPS AND CONTROLS

FIGURE 5

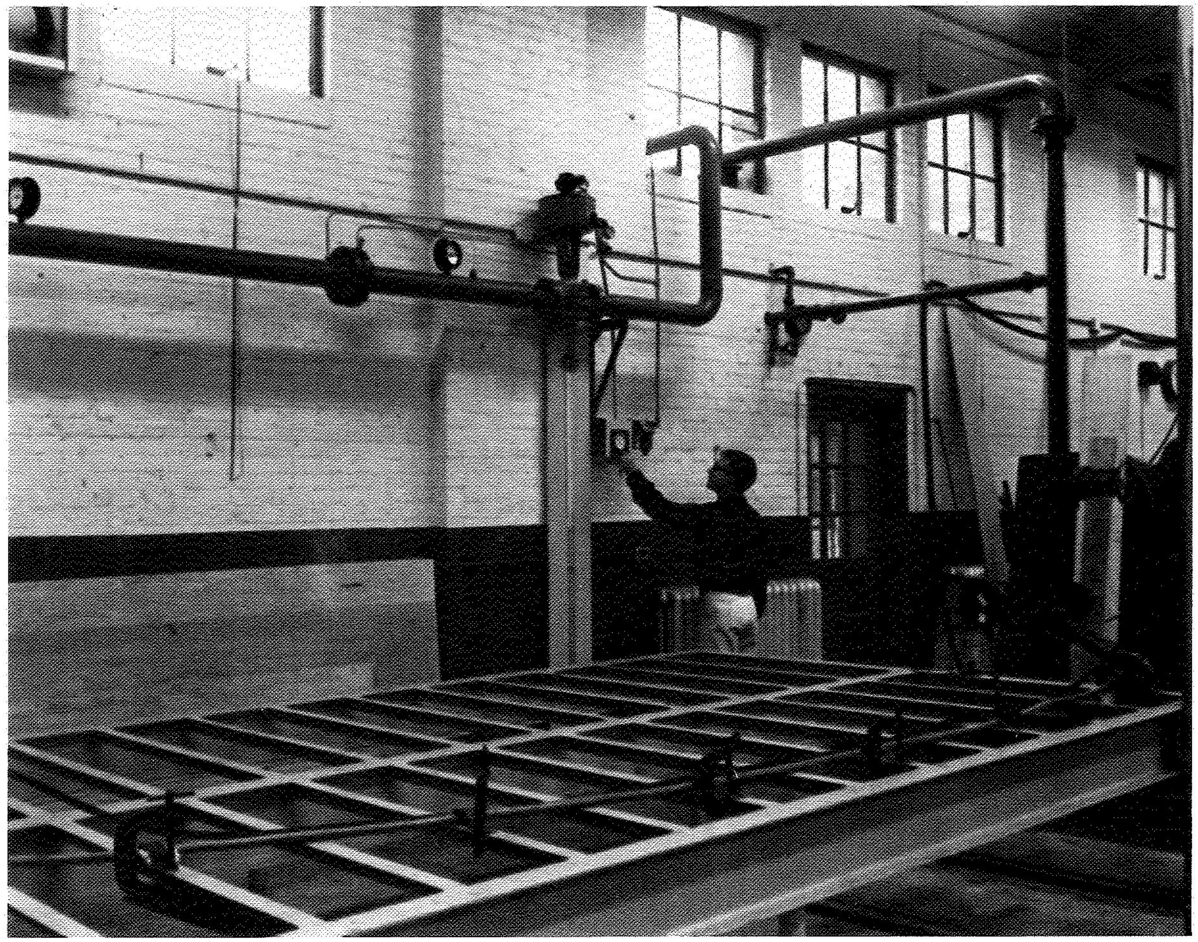

DATA PRODUCTION SYSTEM FOR AIR FIGURE 6.

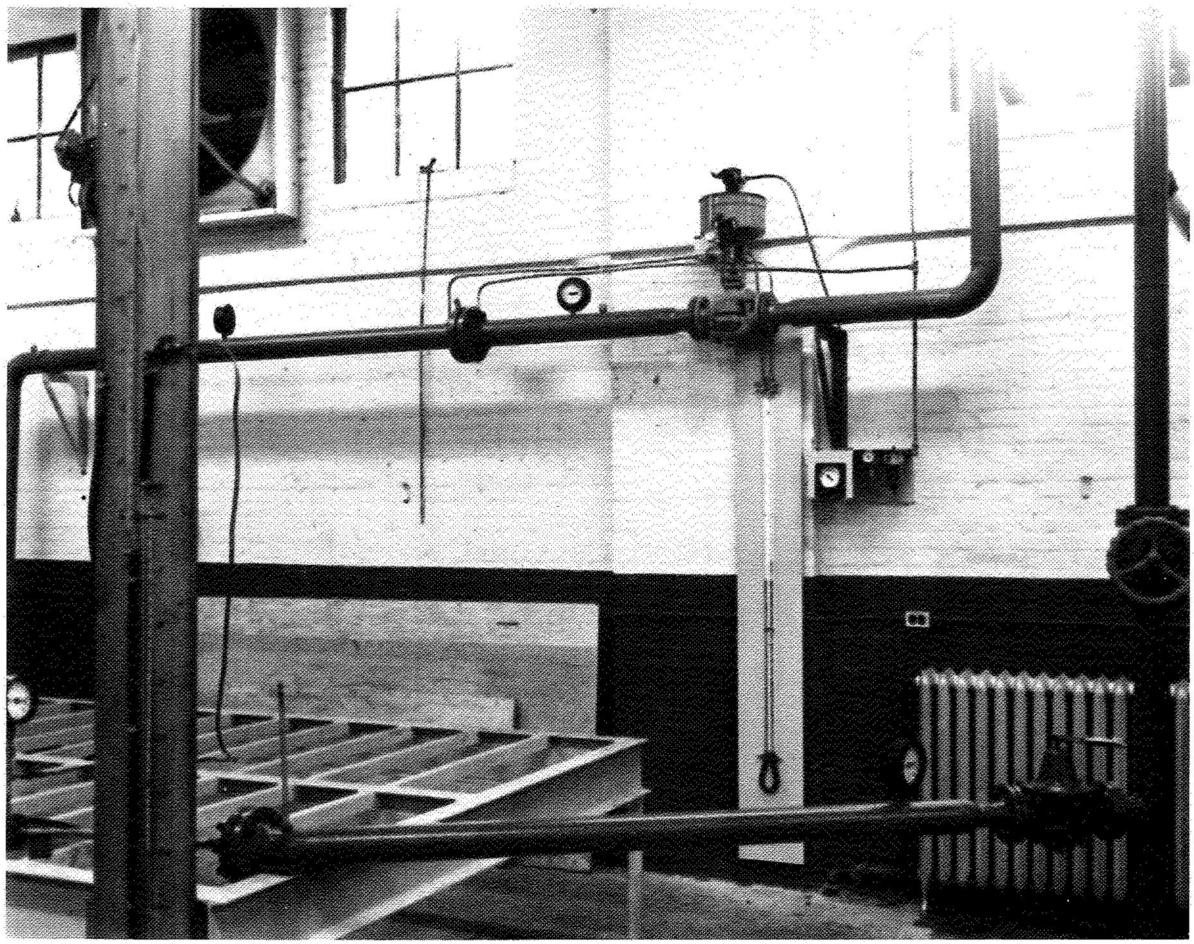

DATA PRODUCTION SYSTEM FOR AIR
SHOWING CONTROLS

FIGURE 7.

FIGURE 8

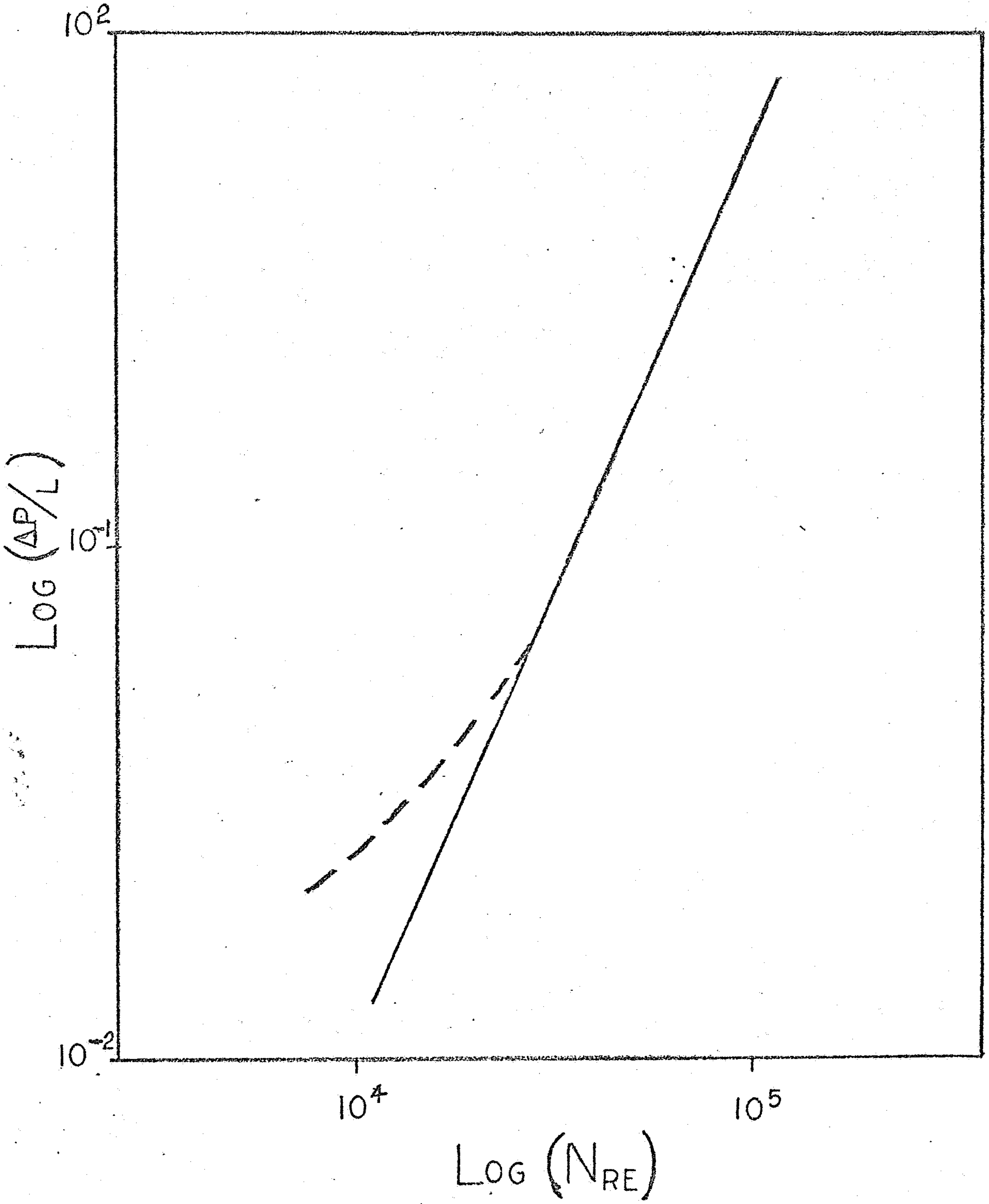

FIGURE 9

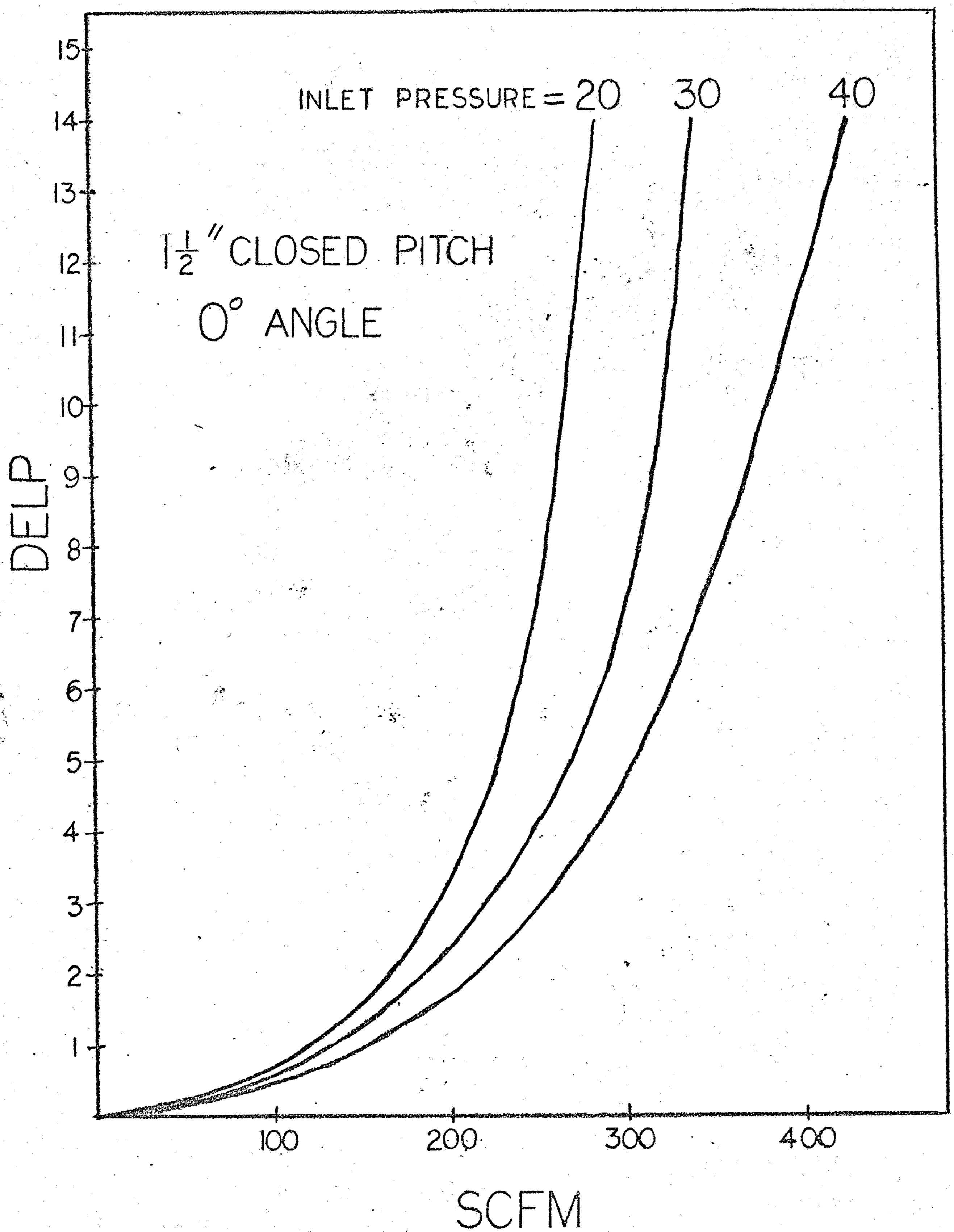

INLET PRESSURE = 20 30 40
1½" CLOSED PITCH
0° ANGLE
DELP
15
14
13
12
11
10
9
8
7
6
5
4
3
2
1
100
200
300
400
SCFM

FIGURE 10

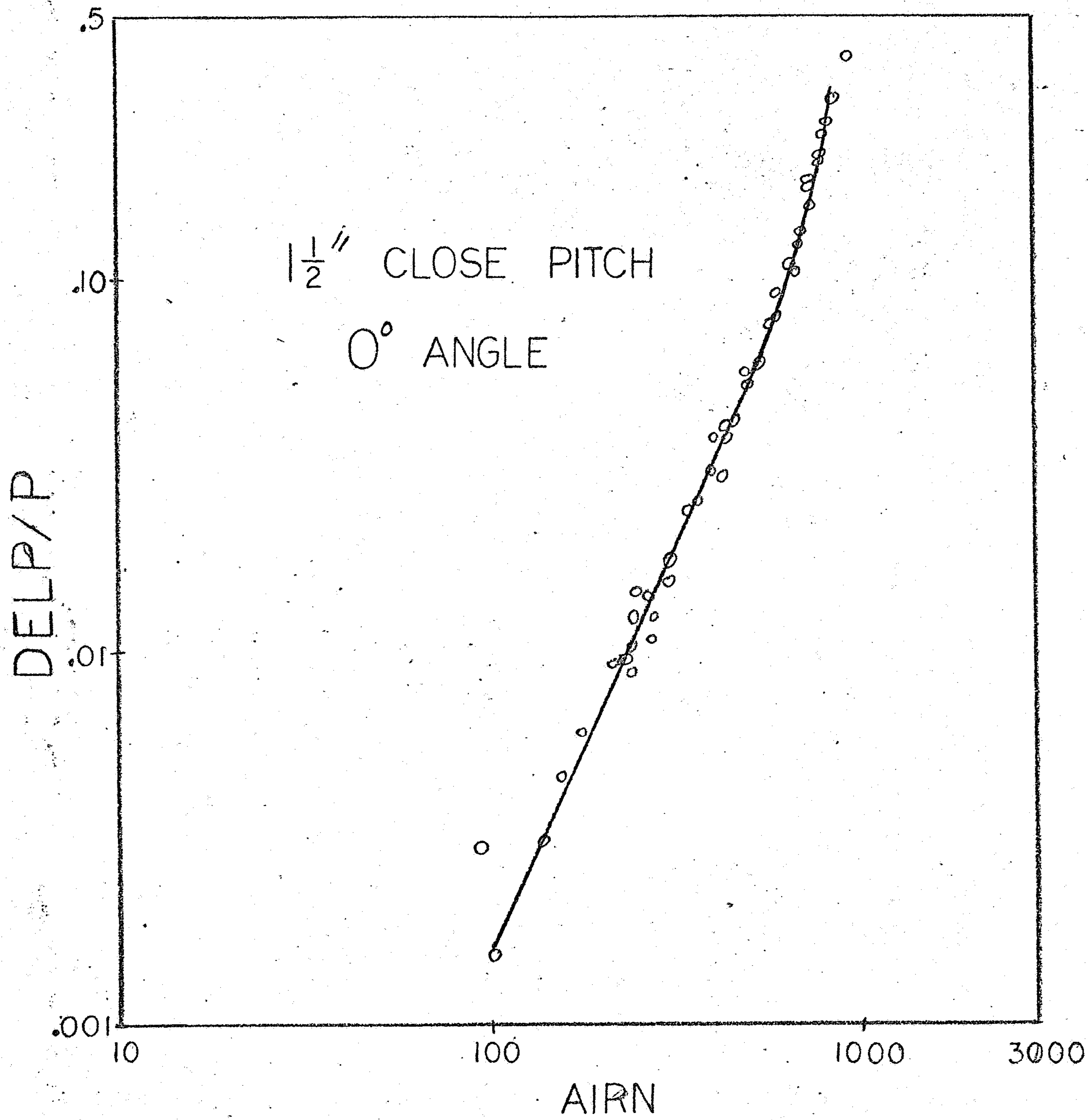

.5
.10
.01
.001
DELP/P
10
100
1000
3000
AIRN
$1\frac{1}{2}$" CLOSE PITCH
0° ANGLE

FIGURE 11

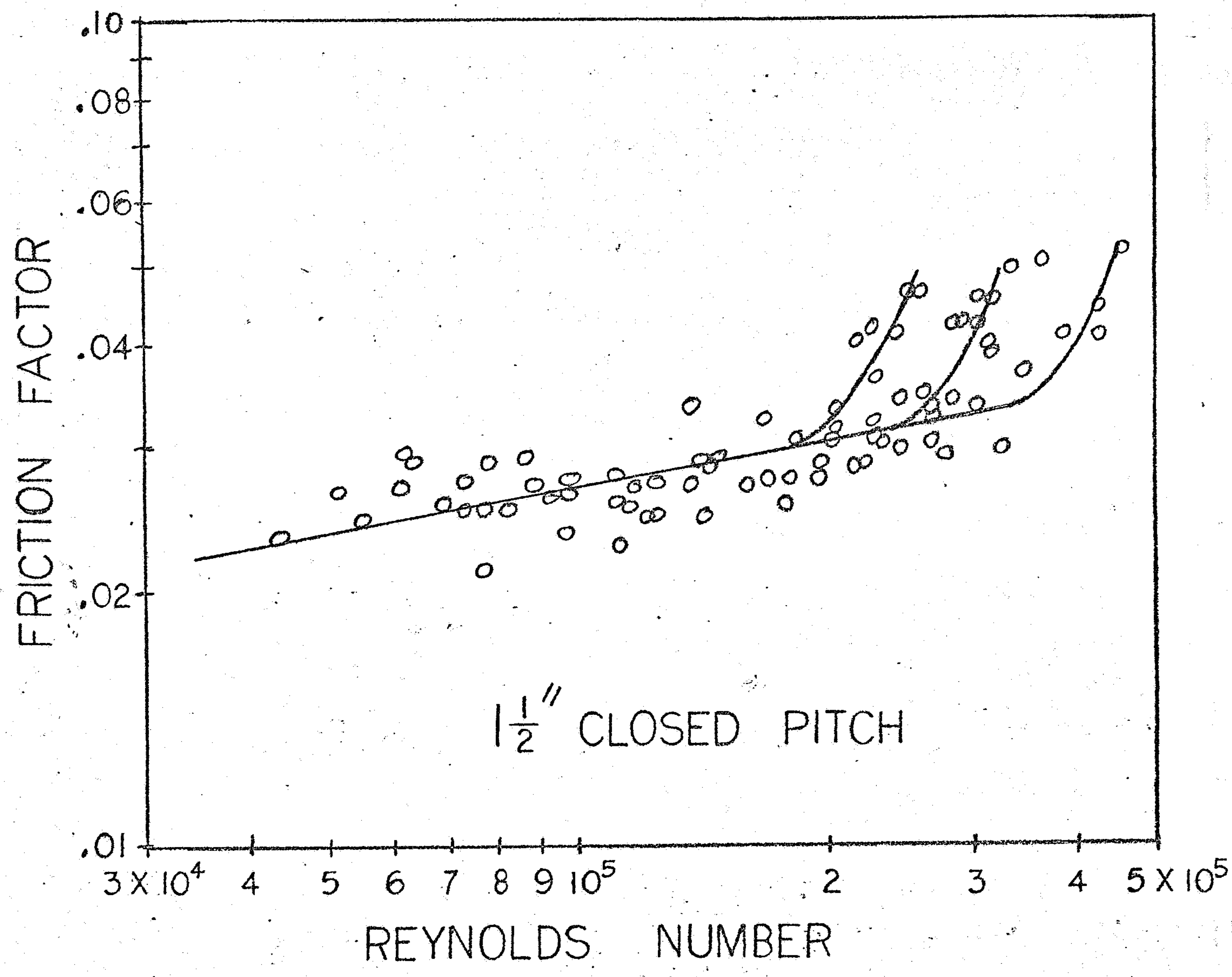

.10
.08
.06
.04
.02
.01
FRICTION FACTOR
$1\frac{1}{2}$" CLOSED PITCH
3 X 10⁴ 4 5 6 7 8 9 10⁵ 2 3 4 5 X 10⁵
REYNOLDS NUMBER

FIGURE 12

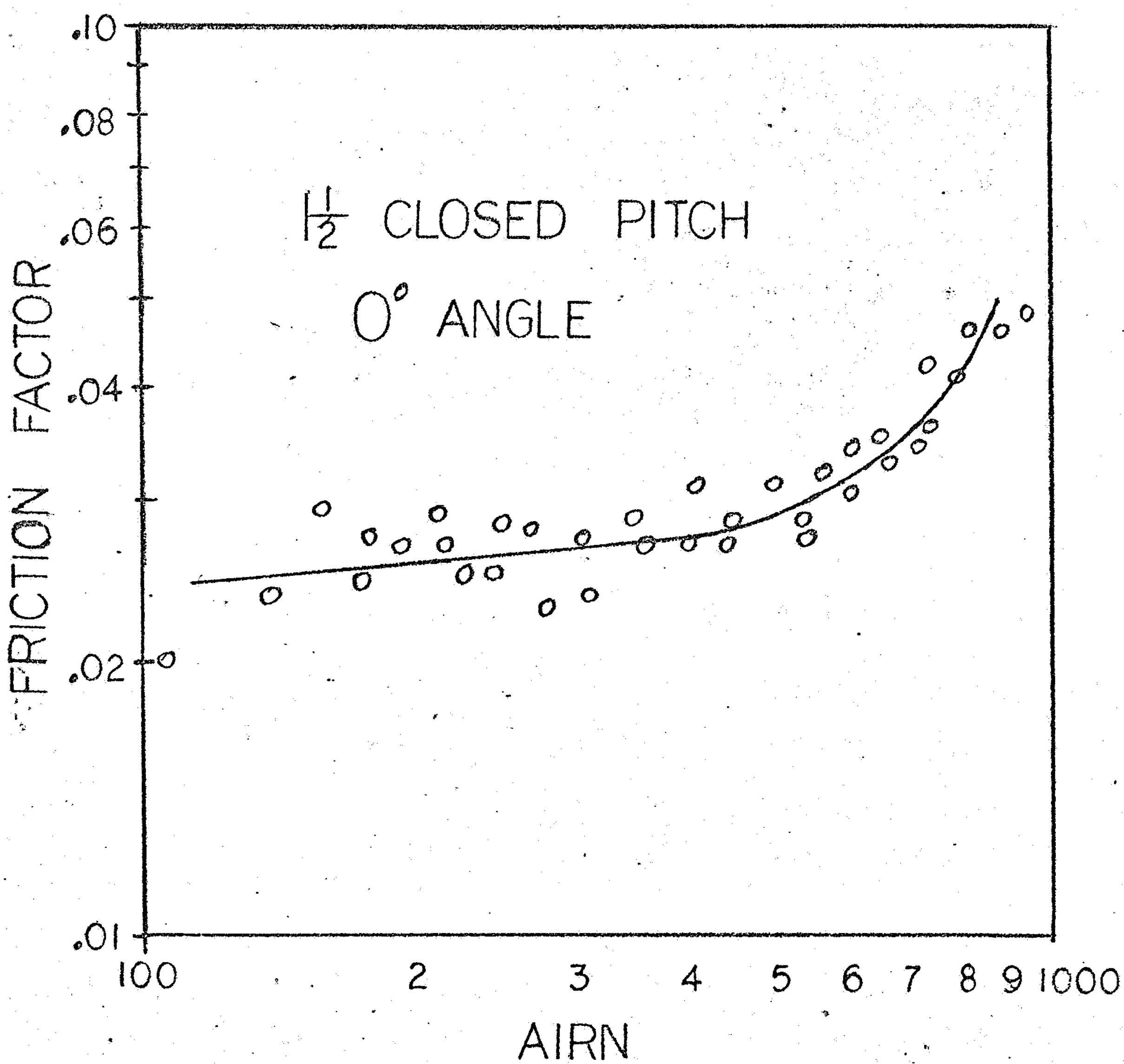

1½ CLOSED PITCH
0° ANGLE
FRICTION FACTOR
.10
.08
.06
.04
.02
.01
100
2
3
4
5
6
7
8
9
1000
AIRN

FIGURE 13

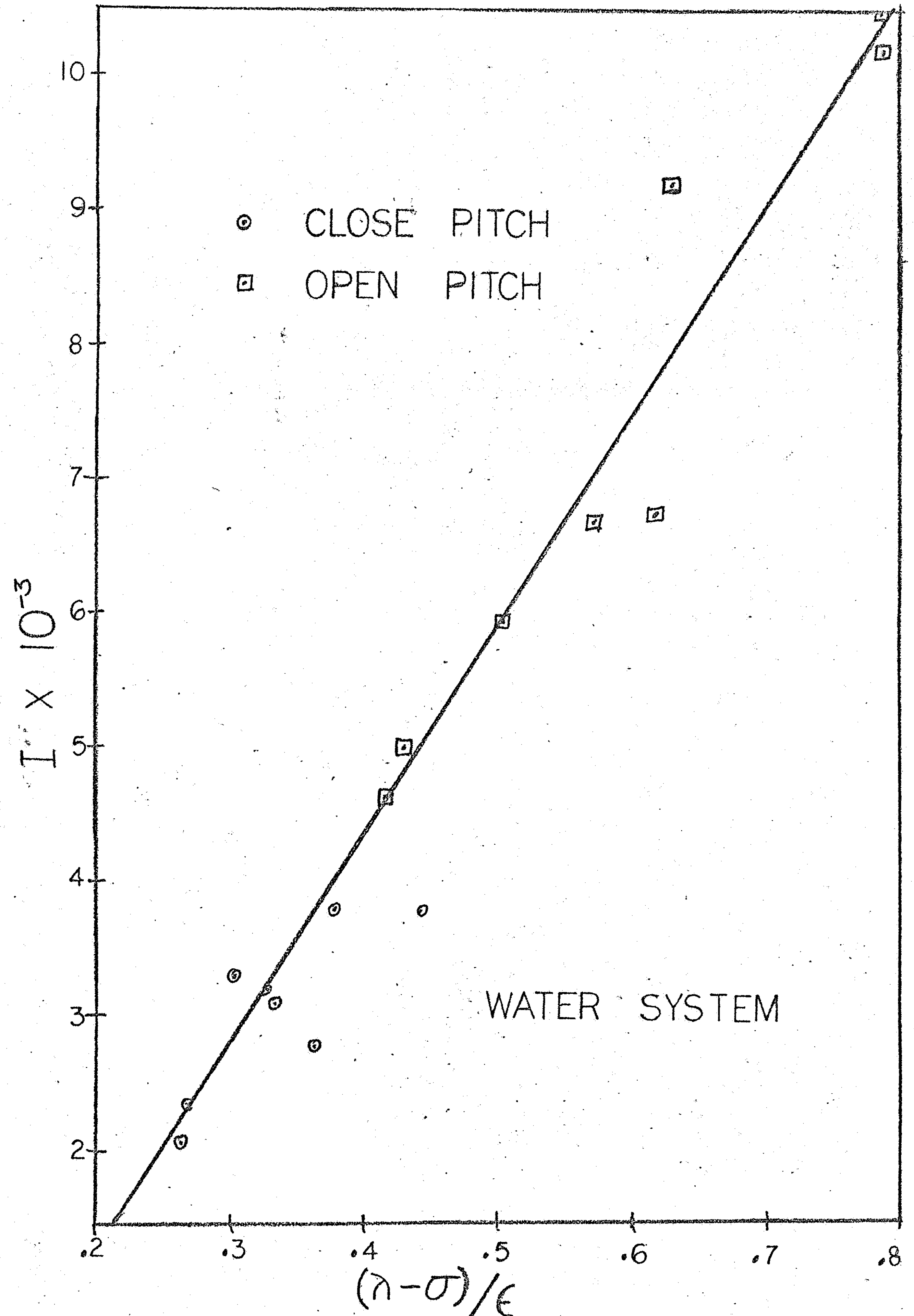
10
9
8
7
6
5
4
3
2
I × 10^-3
CLOSE PITCH
OPEN PITCH
WATER SYSTEM
.2
.3
.4
.5
.6
.7
.8
(λ-σ)/ε

FIGURE 14

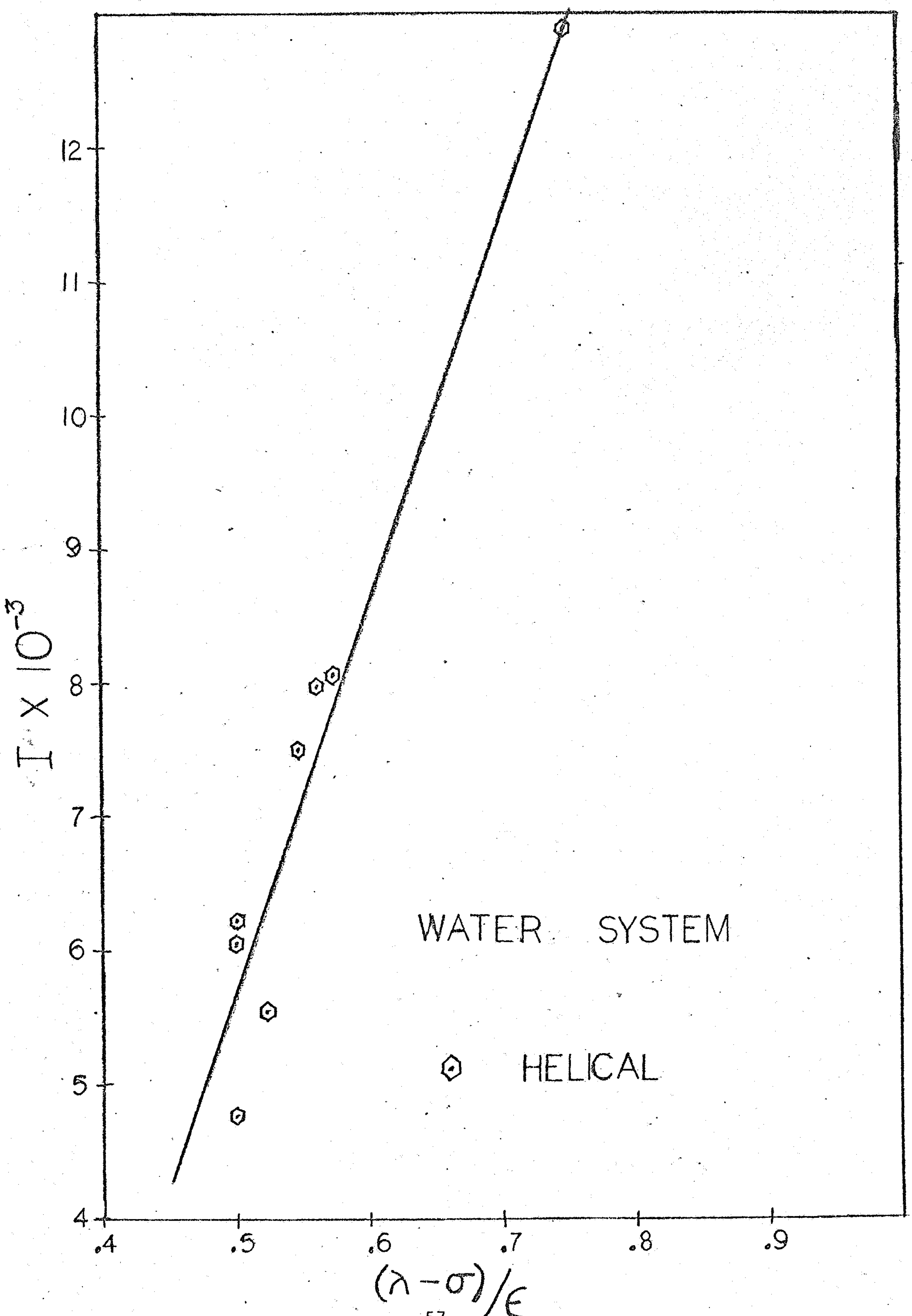

FIGURE 15

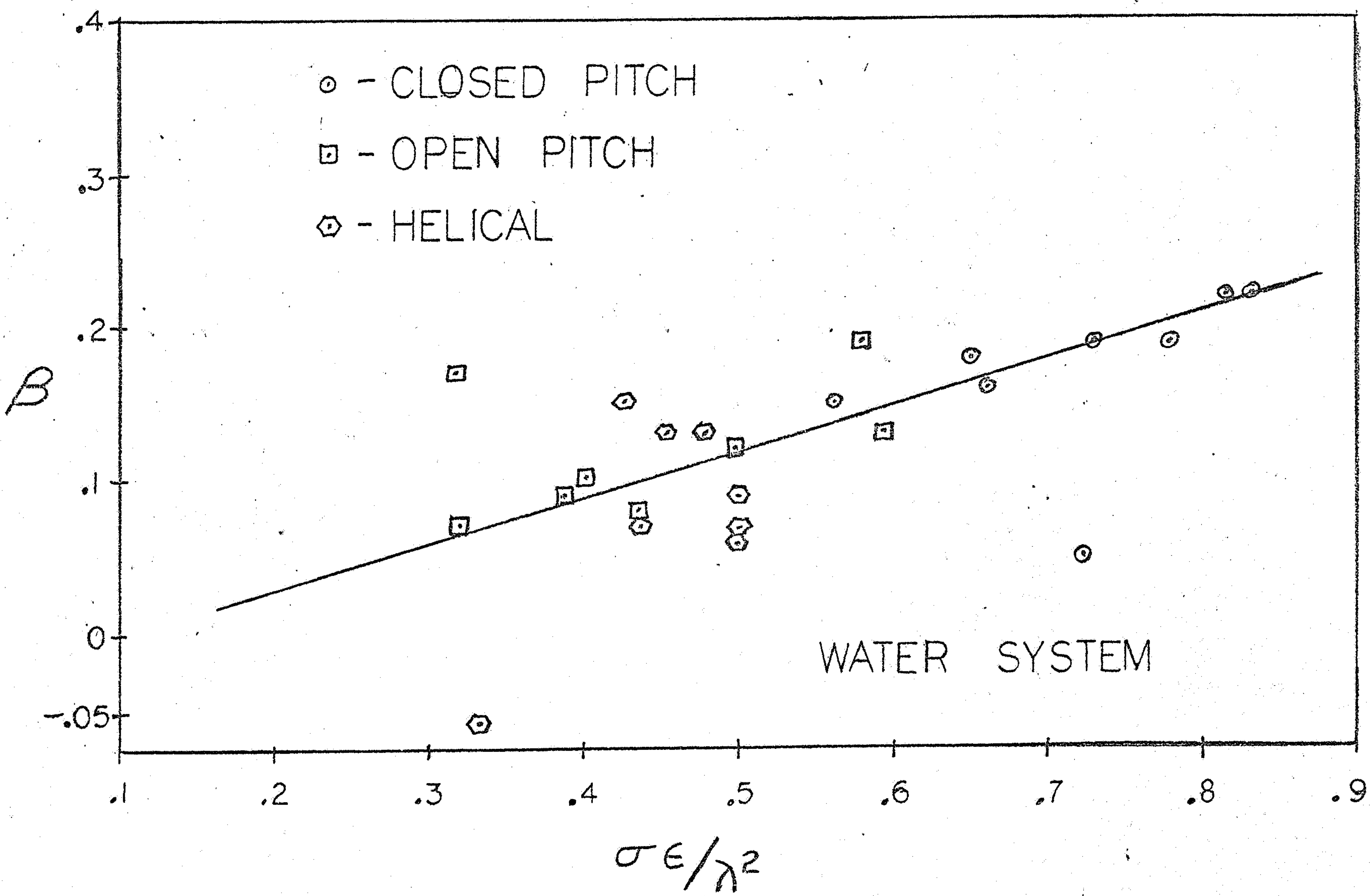

○ - CLOSED PITCH
□ - OPEN PITCH
⬡ - HELICAL
WATER SYSTEM
β
.4
.3
.2
.1
0
-.05
.1
.2
.3
.4
.5
.6
.7
.8
.9
σ ∈/λ²

FIGURE 16

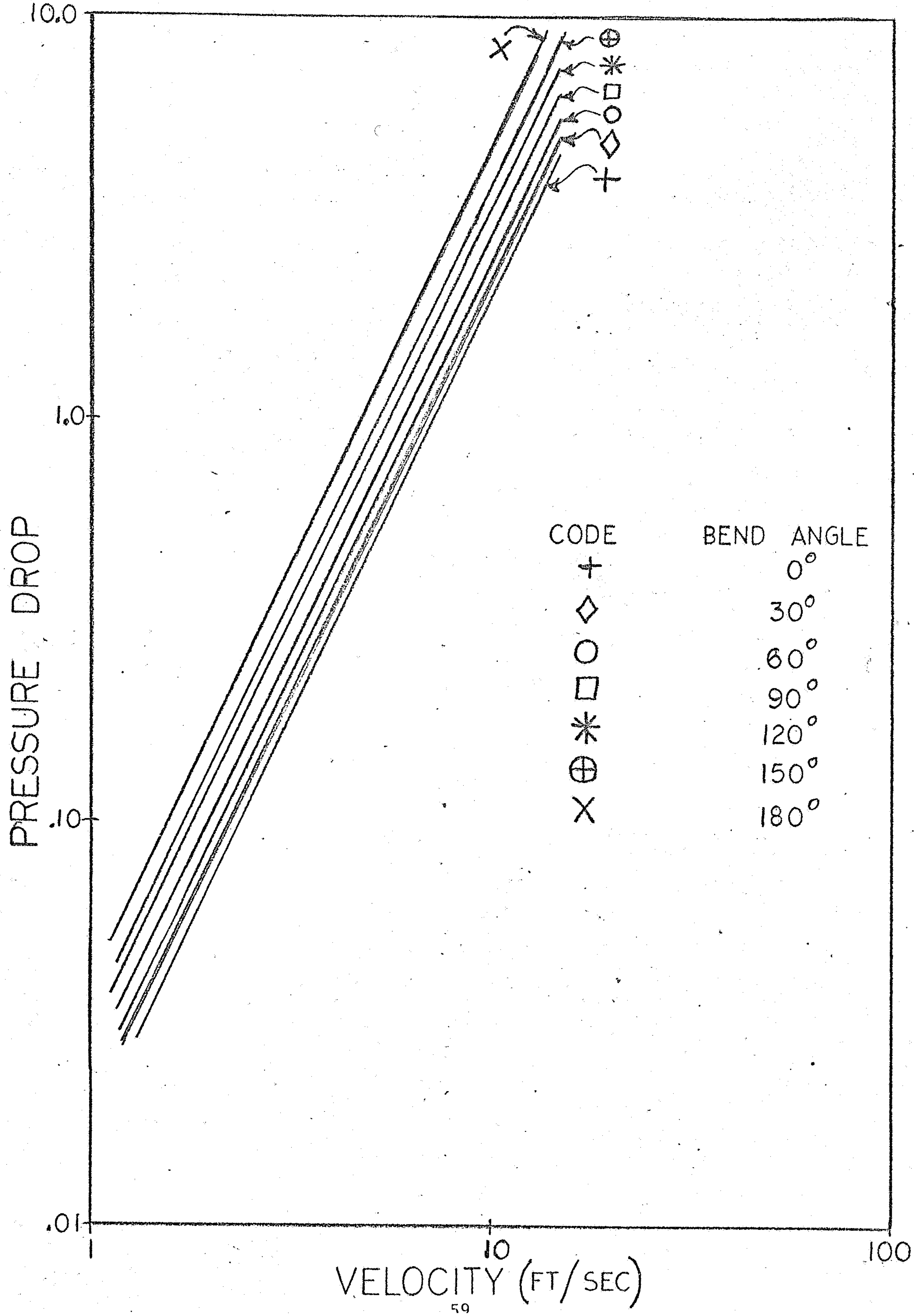

10.0
1.0
.10
.01
1
10
100
PRESSURE DROP
VELOCITY (FT/SEC)
CODE
BEND ANGLE
+ 0°
◊ 30°
○ 60°
□ 90°
✳ 120°
⊕ 150°
X 180°

FIGURE 17

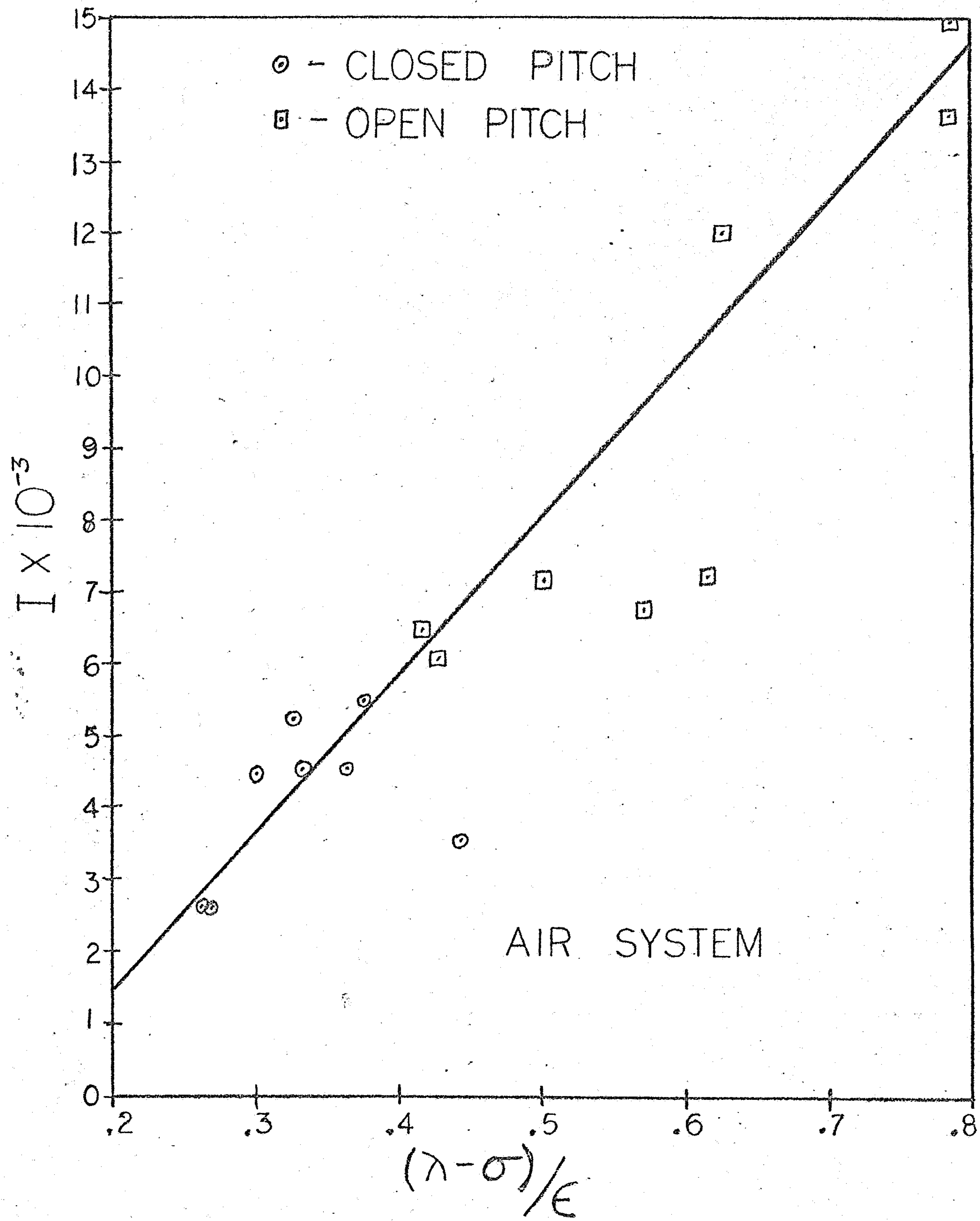

⊙ - CLOSED PITCH
⊡ - OPEN PITCH
AIR SYSTEM
I X 10^-3
15
14
13
12
11
10
9
8
7
6
5
4
3
2
1
0
.2
.3
.4
.5
.6
.7
.8
(λ-σ)/ε

FIGURE 18

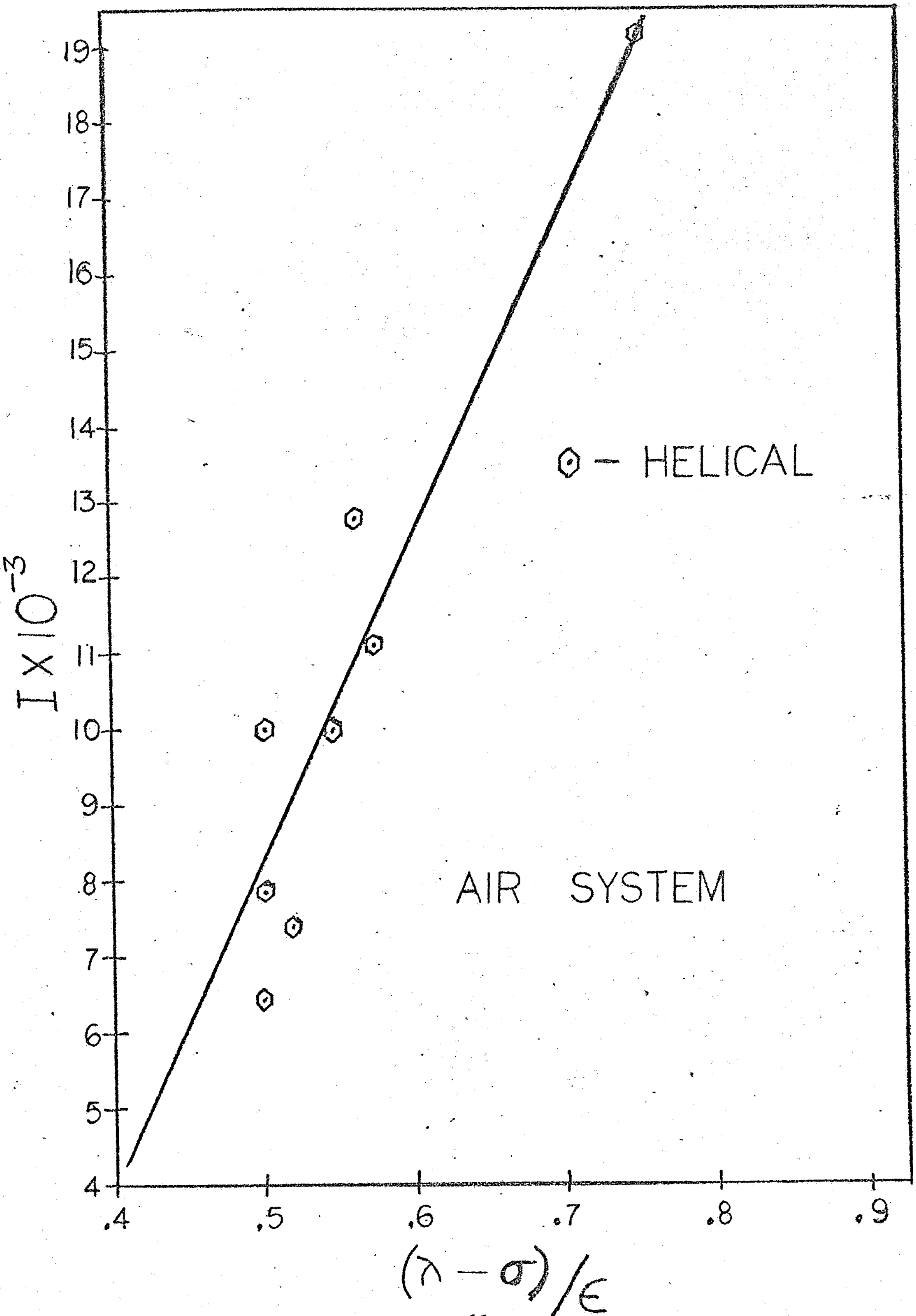

19
18
17
16
15
14
13
12
11
10
9
8
7
6
5
4
I X 10^-3
.4
.5
.6
.7
.8
.9
(λ − σ)/ε
⊙ – HELICAL
AIR SYSTEM

FIGURE 19

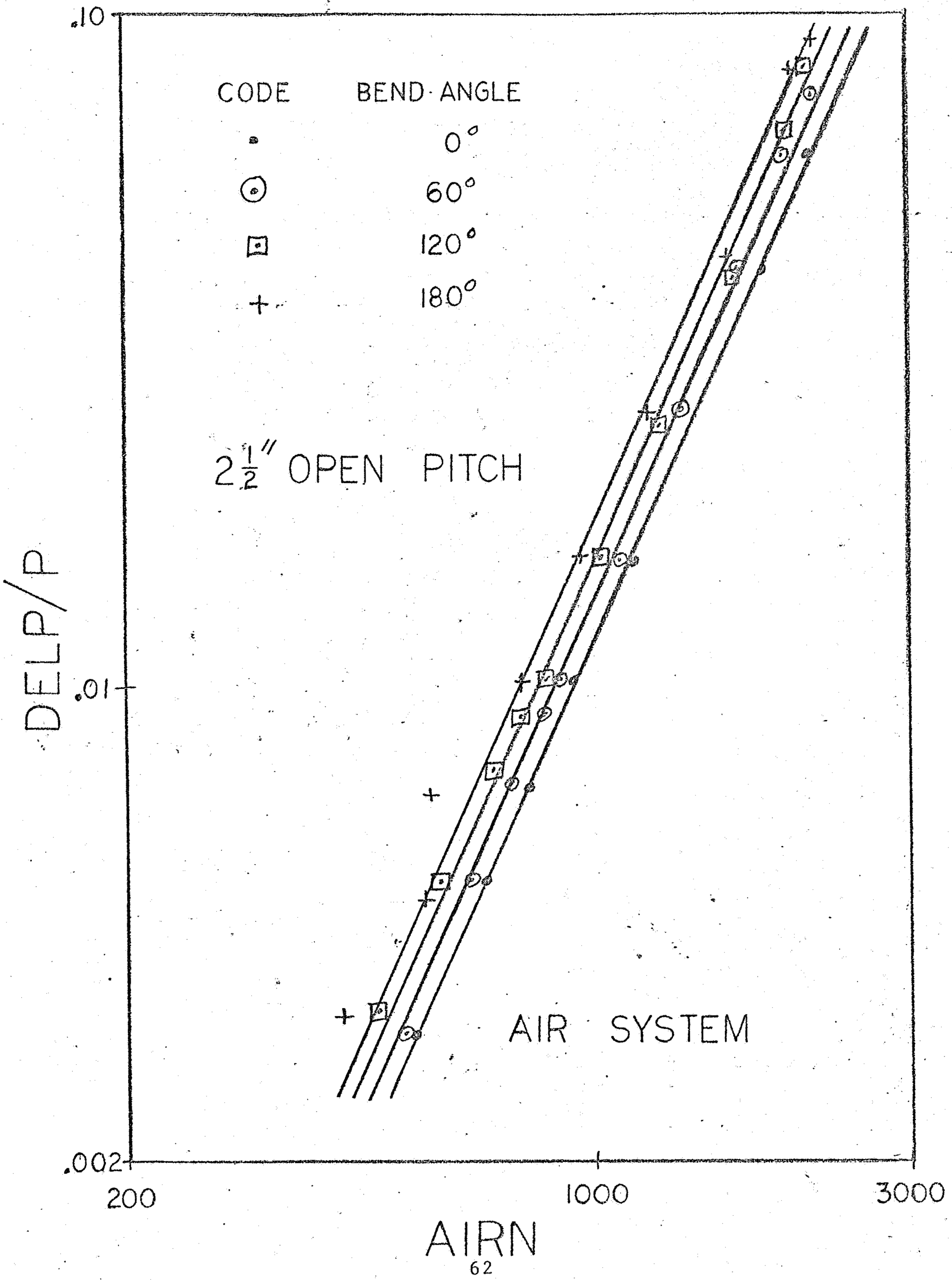
.10
.01
.002
200
1000
3000
DELP/P
AIRN
CODE BEND ANGLE
0°
60°
120°
180°
2 1/2" OPEN PITCH
AIR SYSTEM

Table I

Geometric Parameters

CLOSE PITCH*

ID	λ	ϵ	σ
.551	.125	.156	.0781
.771	.156	.1875	.0937
1.012	.181	.219	.1094
1.266	.1875	.234	.125
1.483	.219	.250	.125
2.046	.250	.297	.172
2.565	.3125	.344	.1875
2.990	.375	.422	.1875

OPEN PITCH

ID	λ	ϵ	σ
.555	.1875	.125	.109
.774	.172	.1875	.09375
1.012	.203	.219	.109
1.255	.219	.219	.109
1.500	.344	.219	.172
2.044	.375	.219	.203
2.535	.406	.328	.21875
3.003	.453	.406	.203

* All measurements given in inches

Table I (con't)

Geometric Parameters

HELICAL

ID	λ	ϵ	σ
.535	.172	.125	.0781
.768	.1875	.1875	.09375
1.061	.250	.250	.1094
1.299	.250	.250	.125
1.560	.3125	.3125	.133
2.081	.344	.344	.156
2.573	.375	.391	.172
3.111	.406	.4375	.1875

Table II

CLOSE PITCH

Diameter	Angle	Ave. Error (%)	Ave. Std. Dev. (%)
1/2	0	-5.7	18.2
	30	2.8	11.3
	60	-10.0	18.1
	90	-11.8	16.8
	120	-9.8	15.7
	150	-14.1	22.2
	180	-3.2	10.6
3/4	0	17.4	24.3
	30	2.3	54.3
	60	6.7	42.0
	90	2.2	45.2
	120	1.5	42.4
	150	5.9	35.4
	180	4.4	30.5
1	0	12.8	15.6
	30	7.0	11.3
	60	6.7	10.9
	90	2.2	8.1
	120	-6.5	13.2
	150	-11.4	20.2
	180	-7.9	13.8

Table II (con't)

CLOSE PITCH

Diameter	Angle	Ave. Error (%)	Ave. Std. Dev. (%)
1 1/4	0	9.8	14.8
	30	15.0	19.1
	60	12.4	17.4
	90	7.0	9.6
	120	-1.3	14.3
	150	2.1	4.2
	180	-3.4	6.5
1 1/2	0	17.2	24.3
	30	13.6	19.5
	60	11.3	13.3
	90	7.9	16.9
	120	3.2	7.9
	150	8.0	13.1
	180	.6	17.0
2	0	21.4	27.5
	30	29.6	49.0
	60	26.5	49.8
	90	28.0	40.7
	120	25.7	33.7
	150	30.0	38.4
	180	24.3	30.7

Table II (con't)

CLOSE PITCH

Diameter	Angle	Ave. Error (%)	Ave. Std. Dev. (%)
2 1/2	0	49.0	54.7
	30	55.8	62.0
	60	45.7	58.7
	90	37.4	47.6
	120	37.4	45.6
	150	39.9	50.6
	180	33.6	43.1
3	0	41.9	45.9
	30	21.8	27.9
	60	24.9	32.3
	90	29.7	35.6
	120	16.8	22.8
	150	19.3	2.48
	180	12.9	31.3

Table II (con't)

OPEN PITCH

Diameter	Angle	Ave. Error (%)	Ave. Std. Dev. (%)
1/2	0	-14.1	21.6
	30	-13.4	33.2
	60	-9.5	17.0
	90	-12.5	19.5
	120	-11.7	19.2
	150	-10.7	25.6
	180	-8.6	20.4
3/4	0	6.4	22.9
	30	1.6	17.1
	60	-15.7	35.8
	90	-9.2	34.2
	120	1.9	7.7
	150	-4.6	15.8
	180	-6.8	20.1
1	0	.6	14.3
	30	-1.2	10.9
	60	-2.1	12.4
	90	10.7	24.9
	120	-8.0	19.0
	150	-7.3	19.1
	180	-13.2	21.8

Table II (con't)

OPEN PITCH

Diameter	Angle	Ave. Error (%)	Ave. Std. Dev. (%)
1 1/4	0	3.8	8.3
	30	4.8	11.5
	60	3.3	8.3
	90	-2.9	11.6
	120	-1.8	19.8
	150	-.79	7.2
	180	-.79	13.5
1 1/2	0	-4.5	23.7
	30	5.1	11.8
	60	9.5	16.2
	90	15.1	19.8
	120	17.6	21.0
	150	15.6	24.7
	180	18.4	24.1
2	0	1.7	15.0
	30	-.18	10.4
	60	1.0	8.5
	90	4.9	12.0
	120	2.5	19.1
	150	-3.1	10.1
	180	-1.1	8.8

Table II (con't)

OPEN PITCH

Diameter	Angle	Ave. Error (%)	Ave. Std. Dev. (%)
2 1/2	0	7.1	13.0
	30	-.34	34.5
	60	11.1	21.6
	90	5.3	30.7
	120	.767	22.7
	150	9.9	18.0
	180	7.5	16.4
3	0	16.5	21.1
	30	20	24.3
	60	37.8	41.6
	90	32.9	37.4
	120	33.2	37.1
	150	29.8	38.0
	180	32.	39.8

Table II (con't)

HELICAL

Diameter	Angle	Ave. Error (%)	Ave. Std. Dev. (%)
1/2	0	.625	12.1
	30	7.96	14.1
	60	6.5	15.3
	90	11.9	17.5
	120	11.9	20.3
	150	12.	33.4
	180	11.5	19.
3/4	0	-1.79	11.7
	30	-9.18	20.9
	60	-7.3	15.4
	90	-7.52	16.3
	120	-5.55	19.5
	150	-.987	12.3
	180	-7.14	16.2
1	0	-1.03	11.1
	30	-1.62	8.51
	60	2.29	6.77
	90	-3.91	12.4
	120	.961	8.26
	150	2.86	6.2
	180	1.11	7.0

Table II (con't)

HELICAL

Diameter	Angle	Ave. Error (%)	Ave. Std. Dev. (%)
1 1/4	0	.252	7.6
	30	5.7	10.37
	60	9.55	12.8
	90	2.73	18.3
	120	3.35	15.1
	150	3.45	14.3
	180	3.55	35.0
1 1/2	0	.386	7.39
	30	1.19	24.2
	60	10.3	16.2
	90	10.2	14.7
	120	8.74	17.7
	150	8.43	16.7
	180	6.98	16.2
2	0	-.261	14.1
	30	.506	30.7
	60	1.94	20.2
	90	5.97	8.87
	120	-4.86	30.6
	150	-7.44	49.4
	180	4.05	8.23

Table II (con't)

HELICAL

Diameter	Angle	Ave. Error (%)	Ave. Std. Dev. (%)
2 1/2	0	13.5	15.6
	30	15.5	19.7
	60	12.7	15.5
	90	16.7	20.7
	120	3.96	7.3
	150	12.	13.5
	180	6.64	11.0
3	0	29.4	32.4
	30	34.6	39.
	60	28.8	34.7
	90	24.4	28.
	120	15.	22.5
	150	22.9	29.0
	180	11.0	40.0

Table III

Air System

Hose	Angle	f/f_o (observed)	f/f_o (predicted)
1 1/4" Helical	60	1.144	1.143
	120	1.297	1.266
	180	1.520	1.382
1 1/2" Helical	60	1.135	1.168
	120	1.285	1.313
	180	1.428	1.450
2 1/2" Helical	60	1.317	1.264
	120	1.617	1.490
	180	1.845	1.705
1 1/4" Close Pitch	60	1.266	1.140
	120	1.543	1.260
	180	1.800	1.374
1 1/2" Open Pitch	60	1.100	1.162
	120	1.196	1.302
	180	1.300	1.435
2 1/2" Open Pitch	60	1.163	1.260
	120	1.310	1.484
	180	1.492	1.696